ISSN2782-4101

INTERNATIONAL JOURNAL of INNOVATIVE MEDICINE

2
2022

‘INTERNATIONAL JOURNAL OF INNOVATIVE MEDICINE’ (IJIM)

Journal’s Website www.ij-im.com
Publishing House Alfmed +7 (495) 616-4800
Box 94, Moscow, 129515, Russia

Editorial Office Office 720, Bldg. 1, 13 Academician Korolev Str., Moscow, Russia
Frequency of publication: 4 issues per year.
Signed for press: 18 April 2022.

Editor-in-Chief of IJIM journal, Doctor of Medical Sciences, Alexander Dolgalev

CONTENTS

DOI:10.33667/2782-4101-2022-2-4-8

THE EFFECT of HIGH-INTENSITY INTERVAL PHYSICAL TRAINING ON THE ENERGY SUPPLY SYSTEM IN PATIENTS AFTER HEART SURGERY

Arzhana Kuular, Teya Kakuchaya, Tamara Dzhitava, Angelina Filatova, Nona Pachuashvili

Federal State Budgetary Institution 'A.N. Bakulev National Research Center for Cardiovascular Surgery' of the Ministry of Health of the Russian Federation (A.N. Bakulev NRCCVS); 135 Rublevskoe Shosse, Moscow, 121552, Russian Federation

SUMMARY

Introduction. *A number of studies have found a reduction in the risk of rehospitalization during cardiorehabilitation after heart surgery. The purpose of the training program for cardiorehabilitation after cardiac surgery is to optimize energy supply systems. Depending on the intensity and duration of the load being performed, energy supply systems 'switch on' in the body.*

Purpose of the study: *to study the effectiveness of the optimal cardiorehabilitation training program on the aerobic energy supply system in cardiac surgery patients.*

Materials and methods. In our study, we examined 47 patients who underwent aortic valve replacement under cardiopulmonary bypass, with an EC duration of 52±20.5 minutes. The patients were divided into two groups: the control group (n=23), who underwent a course of cardiorehabilitation on exercise bikes with constant aerobic training of moderate and medium intensity, at the age of 50.2±3.4 years, and the main group (n=24) – with a course of cardiorehabilitation on exercise bikes with aerobic high-intensity interval physical training, at the age of 51.2±2.8 years (p>0.05). Gender was not taken into account. Anaerobic training was carried out on SCHILLER exercise bikes from day 14 after aortic valve replacement. The load power ranged from 25 to 70–95 watts. Before cardiac rehabilitation, the level of lactate, glucose, pH, pCO2, pO2, BE, lipid profile, BNP in the blood before and after ergometric exercise, data on external respiration, heart rate and blood pressure were assessed. After the course of rehabilitation, the above parameters were evaluated. The duration of the course was 2 weeks.

Results. When evaluating the indicators at the end of the course of cardiorehabilitation was being done, a significant decrease in the controlled parameters after training was observed in both groups, and largely in the group of high-intensity interval physical training than in the group of constant training of medium intensity.

Conclusions. Analysis of the results showed that properly selected parameters of high-intensity interval training could optimize anaerobic glycolysis in patients undergoing operations under cardiopulmonary bypass, as well as increase the functionality of patients. As more and more repetitions of the load are performed, interval training becomes more and more aerobic.

KEYWORDS: *intense physical activity, cardiorehabilitation, anaerobic and aerobic energy supply, artificial circulation*

CONFLICT of INTEREST. *The authors declare no conflict of interest.*

Funding. *Funding for the study was carried out from the personal funds of the authors.*

Introduction

Diseases of the cardiovascular system are the primary health problem and occupy a leading place in the structure of mortality of the population – more than 56% of all deaths, of which about half are deaths from coronary artery disease [1]. The increase in life expectancy of the population is associated with an increase in the prevalence of cardiovascular diseases (CVD) in the population. The increase in the frequency of acquired heart defects (AHD) among patients allowed J.L. d'Arcy et al. consider degenerative heart valve disease as a new cardiac «epidemic» [2]. According to J.M. Takkenberg et al. [3] there is no complete data on the prevalence of PPS in the world. Thanks to the success of cardiac surgery, complex reconstructive operations have become possible for previously inoperable PPS. According to a report in the May 2003 issue of Chest, approximately one in five patients undergoing heart surgery has hyperlactatemia [4]. According to the results of a study by French scientists from the Northern Cardiology Center Saint-Denis, after analyzing 325 patients who underwent heart surgery with artificial circulation, predictors of hyperlactatemia were identified – non-elective surgery, duration of EC, postoperative hyperglycemia and the appointment of adrenaline [4,5]. In many publications, the authors use the dynamics of blood lactate as a criterion for the effectiveness of the therapy and a predictor of a lethal outcome [6]. Patients with high lactate after heart surgery are prone to a large number of postoperative complications, as well as a long stay in the intensive care unit, which leads to significant government costs and a deterioration in the quality of life not only for patients, but also for their families [7]. A large-scale meta-analysis of the Cochran database showed that exercise in patients with coronary artery disease reduces overall mortality by 27%, and mortality from cardiovascular diseases by 31% [8]. Exercise improves oxygen delivery to tissues through vasodilation and angiogenesis, protecting against ischemia-reperfusion injury to the heart, according to Borges J.P. et al. [9]. Aerobic training is accompanied by an increase in the energy capacity of mitochondria not only in skeletal muscles, but also in other tissues; the number of mitochondria and the activity of their enzymes increase; increases tolerance to endurance loads. After exercise, myocardial perfusion improves. One of the possible mechanisms for this is the correction of endothelial function [10]. According to Stanford K.I. et al., Vettor R. et al. enhance mitochondrial biogenesis in adipocytes [11], skeletal muscle myocytes, cardiomyocytes [12], increasing aerobic respiration in these tissues. High-intensity interval training (HIIT), an exercise technique for cardiac rehabilitation, is showing increasing evidence for improved prognosis and health outcomes in patients with cardiovascular disease [13]. Portuguese researchers performed interval intensive training in heart transplant recipients, which showed a significant improvement in VO2peak, heart rate and peak blood pressure after 8–12 weeks after training [14]. Several studies have examined the effect of high-intensity exercise on overall mortality and cardiovascular mortality in cardiac patients. P. Williams et al. [15] reported a gradual decrease in the risk of cardiovascular mortality (–15% per METs-hour /day) in myocardial infarction survivors (n=2377) while running or walking with an exercise level up to 7.2 METs-hour/day. day. There are four main zones of intensity of physical activity, each of which corresponds to a certain level of bioenergetic processes and a range of heart rate:

1) physical activity of low intensity with heart rate less than 75% of its maximum value;
2) physical activity of a supporting nature with a heart rate of 75 to 85% of the maximum heart rate, carried out in the aerobic mode of energy supply;
3) physical activity of a developmental nature with a heart rate of 85 to 95% of the maximum value and a transitional aerobic-anaerobic regime of energy supply;
4) physical activity of submaximal and maximum intensity with a heart rate of more than 95% of the maximum and anaerobic energy supply [16].

The optimal training program is set in two ways: by determining the level of lactate (lactic acid) in the blood or by recording the heart rate (HR) [17]. The predominance of the lactate (anaerobic) energy supply system in patients is a consequence of a decrease in the level of peak oxygen consumption, anemia, the presence of heart failure, and the development of acidosis after heart surgery with EC [18]. To determine the tolerance of aerobic exercise allows the cardiopulmonary test, which measures the maximum oxygen consumption (VO2peak), anaerobic ventilation threshold, the ratio of minute tidal volume (VE) to carbon dioxide release (VCO2), metabolic units (MU) [19]. Without providing energy, the vital activity of the body is impossible, and the more intense the physical load on it, the higher the energy supply should be. The number of publications on the improvement of the aerobic and anaerobic energy supply system of patients after surgery is limited, therefore, new studies are required to evaluate the possibility of the impact of cardiorehabilitation on the energy supply system. Obviously, interval training, like any highly effective technology, can be dangerous if used ineptly [20].

The purpose of the study: to research the effectiveness of the optimal cardiorehabilitation training program on the aerobic energy supply system in cardiac surgery patients/

Materials and methods

In our study, we examined 47 patients who underwent aortic valve replacement under cardiopulmonary bypass, with an EC duration of 52±20.5 minutes. The patients were divided into two groups: the control group (n=23), who underwent a course of cardiorehabilitation on exercise bikes with constant aerobic training of moderate and medium intensity, at the age of 50.2±3.4 years, and the main group (n=24) – with a course of cardiorehabilitation on exercise bikes with aerobic high-intensity interval physical training, at the age of 51.2±2.8 years ($p>0.05$). Gender was not taken into account.

The exclusion criteria were patients with arrhythmias, coronary heart disease, diabetes mellitus, hypo- and hyperthyroidism, hyperthermia, COPD, musculoskeletal diseases, hepatic disorders, CHF III–IV by NYHA, prolonged cardia bypass time (>80 min).

To evaluate the aerobic/anaerobic system, for individual selection of loading power (W) on a bicycle ergometer, the patients of both groups underwent cardiorespiratory test, it differs from the usual exercise tests by the fact that in addition to ECG and blood pressure (BP) during its exercise the parameters of pulmonary gas exchange are recorded through a face mask connected through an airflow transducer to the gas analyzer.

A cardiopulmonary test was carried out before training and at the end of the cardiac rehabilitation course. Cardiorehabilitation training was carried out on SCHILLER ERG-911S/BP (SWITZERLAND) exercise bikes from the 14-th day after the operation, on the background of basic therapy, an hour before lunch, according to the Bruce protocol, every day for 14 days.

In our study, for the main group, we used a high-intensity training scheme that has been proven in terms of safety and effectiveness with 30-second high-intensity training, followed by intermediate 1-minute rest pauses, training was carried out every other day (*Fig. 1*). For the control group, a gradual increase in physical activity by 5–10 W / min until a moderate intensity is reached (*Fig. 2*). During exercise, heart rate, ECG and blood pressure were continuously monitored. The duration of the load increased every day by 2–4 minutes. The following indicators were assessed before and after the exercise cycle: lactate, glucose, pH, pCO2, pO2, BE, lipid profile, BNP, external respiration data (VE/VCO2, FEV1/FVC, VC), heart rate and blood pressure. The concentration of lactate, glucose, pH, CO2, O2, BE in venous blood was measured using a blood analyzer (ABL800 FLEX, Radiometer, Denmark).

Data processing was conducted using Statistica 8.0 applied statistics package. There were used such parametric methods as descriptive statistics – mean value, standard deviation; comparison of two independent samples by non-parametric Wilcoxon-Mann-Whitney criterion. The data were considered statistically significant at p value ≤ 0.05.

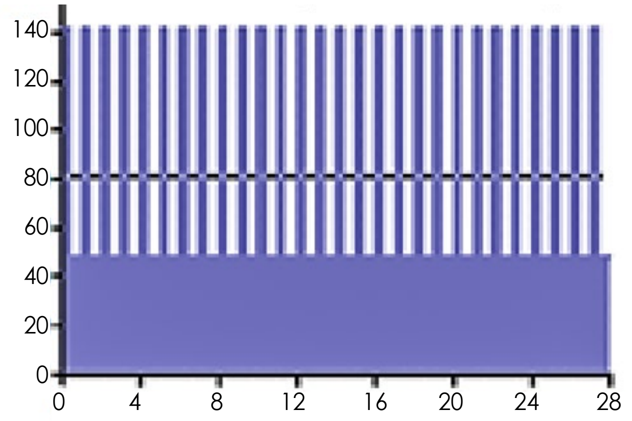

Fig. 1. High intensity interval training.

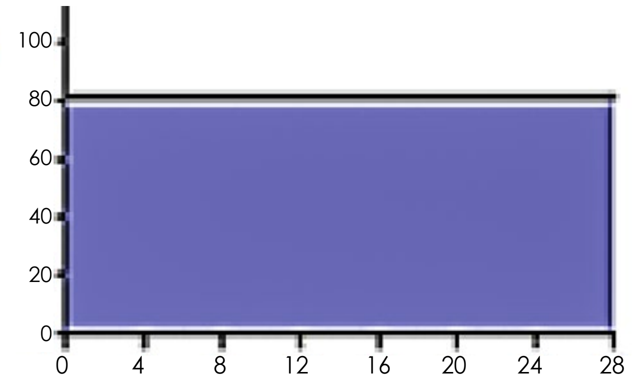

Fig. 2. Constant moderate load intensity.

Results and discussion

Because of the study, according to the cardiopulmonary test in patients after aortic valve replacement under EC conditions, peak oxygen consumption ranged from 17–19 ml / kg / min, which corresponds to the K. Weber classification of moderate CHF, with a VO2peak rate of > 20 ml / kg / min. The presence of heart failure is accompanied by the presence of impaired systolic and diastolic function of the heart, inadequate distribution of blood flow in the peripheral circulation, and in the state after surgery under EC conditions, also muscle detraining [16]. Based on the results of the cardiopulmonary test, patients with a high level of cardiorespiratory training readiness were offered a course of high-intensity interval training every other day, and patients with a low level of exercise readiness and an average risk of developing adverse events were offered only aerobic training at a moderate / medium intensity (consistent training of medium intensity).

To assess patients' cardiorespiratory system we determined several parameters, in particular, peak oxygen consumption (VO2peak), oxygen consumption volume VO2, carbon dioxide excretion volume VCO2, anaerobic threshold (VCO2/VO2=1), minute ventilation (MV), ventilation equivalent VE/VCO2, FEV1/FVC, VC, and cardiorespiratory test time before anaerobic threshold occurred. Gas exchange indices and Mets determined during CPET in the main and control groups were similar (p>0.05) and are presented in *Table 1.*

Analysis of the results showed that properly chosen load ergometric parameters can optimize the anaerobic glycolysis in patients undergoing surgery with cardiopulmonary bypass, as well as increase the functionality of patients.

Table 1

Indices of cardiopulmonary test (M±m)

CPET parameters	Main group	Control group	p
VO2peak, ml/kg/min	17,2±0,5	17,0±0,9	>0,05
VCO2, ml/min	2697±7,5	2710±6,2	>0,05
VE, ml	981±2,0	982±1,7	>0,05
VE/CO2	35,4±0,4	35,5±0,5	>0,05
Mets	6,0±0,6	4,5±0,7	>0,05
FEV1/ FVC,%	67±12	62±14	>0,05
VC, ml	2780±173	2850±155	>0,05
t- CPET, min	8±2,6	5,5±2,7	>0,05

Based on the data shown in *Table 1*, we can note that the moderate decrease of parameters (VO2, FEV1/ FVC, VC) is associated with the surgery under the artificial c

irculation, with temporary respiratory muscle disorder, moderate pain in the sternotomy area, postoperative anemia, tissue hypoxia, and presence heart failure. The time of cardiorespiratory test before the onset of anaerobic threshold in postoperative patients with AC occurs faster, compared with the literature data (15–30 min), indicating the ineffective predominance of anaerobic energy supply system in the patients undergoing cardiac surgery. Under conditions of activation of anaerobic energy supply, an increase in the production of VCO2, ml/min (in the main group – 2697 ± 7.5; in the control group – 2710 ± 6.2), which is a respiratory stimulant, thereby leads to a pathological increase in VE, ml (in in the main group – 981±2.0; in the control group – 982±1.7), respectively, to the rapid achievement of the anaerobic threshold.

The level of blood pressure (SBP and DBP) was almost the same in the groups before training (SBP – p=0.533941; DBP – p=0.107650) and had significant differences after exercise with a more pronounced decrease in the group with intensive training. The comparison of BP data after a course of ergometric exercise revealed a significant decrease in systolic BP after exercise of 145±10,7 mmHg. (p<0,05), which shows the increased number of dilated arterioles in the active muscles, causing a decrease of total peripheral vascular resistance. During physical activity, previously non-functioning skeletal muscle vessels become involved in the blood circulation, and the peripheral blood flow changes in order to supply the increased oxygen demand of the working muscles.

Table 2

Parameters	High-intensity exercise	Regular moderate exercise	p-value
Total cholesterol, mmol/l	3,61±0,70	4,56±0,71	<0,05
High density lipoproteins, mmol/l	1,27±0,24	1,12±0,25	<0,05
Low density lipoproteins, mmol/l	1,93±0,50	1,99±0,55	<0,05
Triglycerides, mmol/l	1,47±0,99	1,45±0,90	<0,05

Serum levels of TG, LDL and HDL are considered the main indicators of lipid metabolism. Serum TG and LDL are a risk factor for atherosclerosis, while HDL is a protective factor. Serum LDL and TG did not clearly change between the two groups, while serum HDL increased slightly in the HIIT group (1.27±0.24 mmol/l) (*Table 2*).

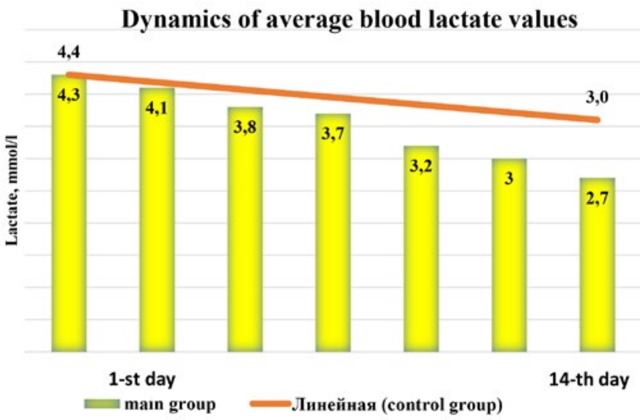

Fig. 3. Dynamics of average blood lactate values on the 14-th day.

Before performing ergometric exercise, both groups underwent blood sampling to determine the following parameters: lactate, glucose, pH, pCO2, pO2, and BE. The generally accepted upper limit of serum lactate is up to 2 mmol/L, but in postoperative patients with AC, in both groups, the average value was 4.4±0.5 mmol/L. Reference values of pO2 in blood were 37–42 mmHg, pCO2–42–55 mmHg, pH=7.32–7.42. Initially, there was a moderate decrease in pO2 (37±4.5 mm Hg) in both groups, the other parameters were within normal limits- pCO2=47±5.5 mm Hg, pH=7.38±0.5. The data of laboratory studies also confirm the predominant function of the lactate energy supply in patients after aortic valve replacement under cardiopulmonary bypass. After a course of ergometric loads on the 14-th day already there were positive dynamics concerning blood lactate concentration in patients in the main group (2.7±0.1 mmol/l) in comparison with the control group (3.0±0.7 mmol/l) (*Fig. 3*).

The data obtained regarding the concentration of lactate in the blood indicates the optimization of aerobic energy supply as a result of exercises on a bicycle ergometer and the correctness of individual selection of power and intensity of aerobic loads. After a course of ergometric loads, the patients underwent a repeated cardiorespiratory test to assess the dynamics of the state of the cardiorespiratory test, aerobic and anaerobic energy supply systems. Relative to the average values of glucose and pH, no significant changes were observed.

According to the obtained data, the selected aerobic cardio load in patients undergoing surgery with CI leads to an increase in the VO2peak value in both groups, in the main group with intense exercise, a more pronounced increase to 21.0±0.9 ml/kg/min ($p<0.05$). An increase in peak oxygen consumption indicates an increase in oxygen transport and utilization, thereby improving the aerobic energy supply mechanism. The improved ventilatory function of the lungs is shown by the vital capacity of the lungs (VC). This value after training in the main group increased up to 3350±133 ($p>0,05$) compared to the control group –3180±173. VC is an important parameter of functional abilities of the system of external respiration, and also indirectly specifies the maximum area of a respiratory surface of lungs, which provides gas exchange.

Table 3

Dynamics of CPET indicators after a course of ergometric loads in both groups

CPET parameters	Control group	Main group	p
VO2peak, ml/kg/min	19,05±0,6	21,0±0,9	<0,05
VCO2, ml/min	2807±8,5	2800±8,0	>0,05
VE, ml	920±2,1	870±1,4	>0,05
VE/CO2	34,4±0,4	32,5±0,4	>0,05
Mets	6,0±0,9	7,8±0,4	<0,05
FEV1/ FVC	67±12	75±10	>0,05
VC	3180±173	3350±133	>0,05
t- CPET, min	11±2,6	14,5±2,7	<0,05

The course of the cardiorehabilitation program in both groups increased the performance of the cardiovascular system in patients after surgery with EC: the metabolic equivalent significantly increased in the control group to 6.0±0.9, and in the main group to 7.8±0.4 ($p< 0.05$).

Significant changes are observed regarding the time to reach the anaerobic threshold, the VE / VCO2 coefficient, which proves the acceleration of blood flow with regular aerobic exercise, the improvement of endothelial function and increases the number of mitochondria in the muscles, accelerates lipolysis, thereby increasing the body's need for oxygen.

BNP levels are elevated in patients with left ventricular dysfunction. At the same time, the content of BNP in blood plasma significantly correlates with the functional classes of chronic heart failure. Determining the level of BNP in blood plasma helps to assess the severity of chronic heart failure, predict the further development of the disease, and also evaluate the effect of ongoing therapy. The guidelines of the Association of Pediatric Cardiologists of Russia for the diagnosis and treatment of chronic heart failure in children and adolescents (2010) determined that BNP more than 100 pg/ml is associated with congestive heart failure [02]. In our patients after aortic valve replacement, BNP averaged 95.1±15 pg/mmol. After completing the course of ergometric loads in both groups, there was a downward trend, but mainly in the group with intense loads.

Conclusions

Analysis of the results showed that properly selected parameters of ergometric loads could optimize aerobic glycolysis in patients undergoing operations under cardiopulmonary bypass, as well as improve their clinical condition. During the implementation of a rehabilitation program with aerobic exercise, the patient's self-confidence increases, self-esteem increases, anxiety and depression decrease [23]. Physical exercise on a bicycle ergometer activates the activity of the cardiorespiratory system in patients undergoing heart surgery under EC conditions, accelerates blood flow, leading to an increase in metabolism. Intensive interval training triggers metabolic changes in the body, which is reflected in the mechanism of fat oxidation, a decrease in lipid profile. Leading cardiology societies in North America and Europe recommend that patients switch from moderate physical training to more intense interval training to improve the quality of life [24]. The uniqueness of the energy supply system lies in the fact that it can be optimized at any age, which makes it possible to use ergometric loads for patients after heart surgery. For this, it is necessary to use the selected parameters of the training program. Constant high-intensity interval loads, with the right selected regular mode, are equated to constant moderate loads, and even have an advantage in some indicators. Meta-analyses have found superiority of high- and moderate-intensity high-intensity training over continuous moderate-intensity training in terms of cardiovascular performance [25] and increased VO2 peak.

References

1. L. A. Bokerija. Aktual'nye voprosy razvitija serdechno-sosudistoj i rentgenojendovaskuljarnoj hirurgii v Rossijskoj Federacii/ L. A. Bokerija, I. N. Stupakov, R. G. Gudkova*, I. A. Jurlov, Ju. M. Botnar', V. M. Vatolin // Bjulleten' NCSSH im. A. N. Bakuleva RAMN-2012; 13(5).34–40
2. Goldbarg S. H., Elmariah S., Miller M. Fuster V. Insights Into Degenerative Aortic Valve Disease // J Am Coll Cardiol. 2007. Vol. 50, № 13. P. 1205–1213.
3. Prevalence, Referral Patterns, Testing, and Surgery in Aortic Valve Disease: Leaving Women and Elderly Patients Behind? / Bach D. S. and others // The Journal of Heart Valve Disease. 2007. Vol.
4. Associacija serdechno-sosudistyh hirurgov Rossii, Vserossijskoe nauchnoe obshhestvo kardiologov, vserossijskoe nauchnoe obshhestvo intervencionnyh radiologov i rentgenjendovaskuljarnyh hirurgov. Pokazanija k revaskuljarizacii miokarda (Rossijskij soglasitel'nyj dokument)- M.: NCSSH im. A. N. Bakuleva RAMN, 2011.– 162 s.
5. Maillet J-M, LeBesnerais P, Cantoni M, Nataf P, Ruffenach A, Lessana A, et al. Frequency, risk factors, and outcome of hyperlactatemia after cardiac surgery. Chest. 2003. Vol. 123. P. 1361–1366
6. Laktat v krovi cheloveka. Znachenie issledovanija. Interpretacija rezul'tatov. http://labix.com.ua/files/1379078313.pdf. (data obrashhenija 2 avgusta 2017)
7. N. V. Gal'ceva. Reabilitacija v kardiologii i kardiohirurgii. Klinicist.2015; 2. 13–22.
8. Heran B. S., Chen J. M., Ebrahim S. et al. Exercise-based rehabilitation for coronary heart disease. Cochrane Database Syst Rev 2011;7: CD001800.
9. Borges J. P., da Silva Verdoorn K. Cardiac ischemia/reperfusion injury: the beneficial effects of exercise. Advances in Experimental Medicine and Biology. 2017; (999): 155–179.
10. Carvalho M. N., Colaco A. L., Fortes Z. B. Cytokines, endothelial dysfunction, and insulin resistance // Arq. Bras. Endocrinol. Metabol.– 2006.– Vol. 502.– P. 304–312.
11. Stanford K. I., Goodyear LJ. Exercise regulation of adipose tissue. Adipocyte. 2016; (5): 153–62. https://doi.org/10.1080/21623945.2016.1191307
12. Vettor R., Valerio A., Ragni M., Trevellin E., Granzotto M., Olivieri M. et al. Exercise training boosts eNOS-dependent mitochondrial biogenesis in mouse heart: role in adaptation of glucose metabolism. American Journal of Physiology-Endocrinology and Metabolism. 2014; (306): E519–28. https://doi.org/10.1152/ajpen-do.00617.2013
13. Yu AKD, Kilic F, Dhawan R, Sidhu R, Elazrag SE, Bijoora M, Sekhar S, Makaram Ravinarayan S, Mohammed L. High-Intensity Interval Training Among Heart Failure Patients and Heart Transplant Recipients: A Systematic Review. Cureus. 2022 Jan 17;14(1): e21333. doi: 10.7759/cureus.21333. PMID: 35186591; PMCID: PMC8849491.
14. Perrier-Melo RJ, Figueira FAMDS, Guimarães GV, Costa MDC. High-Intensity Interval Training in Heart Transplant Recipients: A Systematic Review with Meta-Analysis. Arq Bras Cardiol. 2018 Feb;110(2):188–194. doi: 10.5935/abc.20180017. Epub 2018 Feb 19. PMID: 29466487; PMCID: PMC5855913.
15. Williams PT, Thompson PD. Increased cardiovascular disease mortality associated with excessive exercise in heart attack survivors. Mayo Clin Proc. 2014;89:1187–94. doi: 10.1016/j.mayocp.2014.05.006
16. Kakuchaya Tea Tamazovna, Jitava Tamara Georgievna, Pachuashvili Nona Vazhaevna, Kuular Arzhana Makarovna, Domracheva Irina Ivanovna, Zakaraya Nino Eldarievna COMPARATIVE ANALYSIS of HIGH AND MODERATE INTENSITY AEROBIC CARDIORESPIRATORY TRAINING IN PATIENTS WITH CARDIAC SURGERY. 2021. № 4. URL: https://cyberleninka.ru/article/n/sravnitelnyy-analiz-aerobnyh-kardiorespiratornyh-trenirovok-vysokoy-i-umerennoy-intensivnosti-u-bolnyh-kardiohirurgicheskogo (Date of access: 07/31/2022).
17. Jansen Peter.Ya65 Heart rate, lactate and endurance training: Per. from English.– Murmansk: Tuloma Publishing House, 2006.– 160 p.
18. A. M. Kuular, T. T. Kakuchaya, T. G. Jitava, A. G. Filatova, L. K. Nartikoeva, N. O. Vasyukova, N. V. Pachuashvili. Influence of bicycle ergometric loads on the energy supply system in patients after surgery with cardiopulmonary bypass. Bulletin of the NCSSH them. A. N. Bakuleva RAMS. 2018; 19(4): 480–486. DOI: 10.24022/1810–0694–2018–19–4–480–486
19. Beaver W. L., Wasserman K., Whipp B. J. Online computer analysis and breath-by-breath graphical display of exercise function tests. J. Appl. Physiol. 1973; 34 (1): 128–32.
20. https://lifehacker.ru/chemu-mogut-navredit-viit/
21. Kerbikov, O., et al. "Cardiopulmonary Exercise Testing in Clinical Practice." Clinical Practice, 2012, p. 62. (in Russian)
22. Basargina E. N., Leonteva I. V., Kotlukova N. P., Kovalev I. A., Sharykin A. S. Diagnosis and treatment of chronic heart failure in children and adolescents: guidelines. Available from: http://www.cardio-rus.ru/doc/metod_rekom_2010.pdf. (accessed: 10.08.2016) (In Russ.)
23. Fokin V. F., Ponomareva N. V. Energy physiology of the brain. Moscow: «ANTIDOR», 2003. 288 p.
24. Belardinelli R, Georgiou D, Cianci G, Purcaro A. 10-year exercise training in chronic heart failure: a randomized controlled trial. J Am Coll Cardiol. 2012;60(16):1521–8. DOI:10.1016/j.jacc.2012.06.036
25. High-intensity interval training (HIT) for effective and time-efficient pre-surgical exercise interventions / M. Weston, K. L. Weston, J. M. Prentis, C. P. Snowden // Perioperative Medicine.– 2016.– Vol. 5.– P. 1.

Received 10.05.2022
Revised 18.05.2022
Accepted 20.05.2022

INFORMATION ABOUT AUTHORS

Kuular Arzhana Makarovna, *Candidate of medical sciences, junior assistant of the department of Cardiac Surgery and Rehabilitation of Adult Patients with Cardiac Pathology of the Federal State Budgetary Institution 'A. N. Bakulev National Research Center for Cardiovascular Surgery' of the Ministry of Health of the Russian Federation (A. N. Bakulev NMRCVS), Moscow, Russian Federation. ORCID: https://orcid.org/0000-0002-2133-9674. Tel. +79777238627, e-mail: lebed8507@mail.ru*

Kakuchaya Teya Tamazovna, *MD, Head of the department of Cardiac Surgery and Rehabilitation of Adult Patients with Cardiac Pathology of the Federal State Budgetary Institution 'A. N. Bakulev National Research Center for Cardiovascular Surgery' of the Ministry of Health of the Russian Federation (A. N. Bakulev NMRCVS), Moscow, Russian Federation. ORCID: https://orcid.org/0000-0001-9383-2073*

Dzhitava Tamara Georgievna, *Candidate of medical sciences, Assistant manager of the department of Cardiac Surgery and Rehabilitation of Adult Patients with Cardiac Pathology of the Federal State Budgetary Institution 'A. N. Bakulev National Research Center for Cardiovascular Surgery' of the Ministry of Health of the Russian Federation (A. N. Bakulev NMRCVS), Moscow, Russian Federation. ORCID: https://orcid.org/0000-0002-6141-22-31. Tel. +79031285534, e-mail: tgdjitava@mail.ru*

Filatova Angelina Gennadievna, *cardiologist, Federal State Budgetary Institution 'A. N. Bakulev National Research Center for Cardiovascular Surgery' of the Ministry of Health of the Russian Federation (A. N. Bakulev NMRCVS). ORCID: https://orcid.org/0000-0001-5070-2447. Tel. +79265436204, e-mail: agfilatova@mail.ru*

Pachuashvili Nona Vazhaevna, *Cardiologist, Postgraduate student of the department of Cardiac Surgery and Rehabilitation of Adult Patients with Cardiac Pathology of the Federal State Budgetary Institution 'A. N. Bakulev National Research Center for Cardiovascular Surgery' of the Ministry of Health of the Russian Federation (A. N. Bakulev NMRCVS), Moscow, Russian Federation. Tel. +79299372539, e-mail: pachuashvili.nona@mail.ru*

DOI:10.33667/2782-4101-2022-2-9-11

THE CHOICE OF A PERSONALIZED METHOD IN THE DIAGNOSTICS OF BREAST CANCER IN A CYST BY MEANS OF HYBRID TECHNOLOGIES UNDER ULTRASOUND NAVIGATION

Mariam Arabachyan[1,2,3], Alexey Borsukov[1,3]

[1]Federal State Budgetary Educational Institution of Higher Education «Smolensk state medical university» of the Ministry of Health of the Russian Federation, Smolensk, Russian Federation
[2]Regional State Budgetary Health Institution «Smolensk Regional Oncological Clinical Dispensary», Smolensk, Russian Federation
[3]The Problem Research Laboratory «Diagnostic investigations and minimally invasive technologies», Smolensk State Medical University, Ministry of Health of Russia Smolensk, Russian Federation

SUMMARY
The article presents the results of the use of a new improved method of cytologic diagnostics of cancer in a breast cyst by applying hybrid technologies. By using our new created method with the application of ozone-oxygen mixture, unlike the traditional method of fine needle aspiration biopsy of breast cysts with a solid parietal component, the probability of obtaining unaltered atypical cells in the punctate in the presence of malignization increases, thereby promoting the informativeness and sensitivity of this diagnostic method.

KEYWORDS: *breast cancer, fine needle aspiration biopsy, ozone-oxygen mixture, intracystic cancer, ultrasonic navigation.*

CONFLICT of INTEREST. *The authors declare no conflict of interest.*

Introduction

Breast cancer (BRCA) currently occupies a leading place in the structure of oncological morbidity of the female population, both in Russia and around the world [1, 7]. More than 2 million newly diagnosed cases of this disease are detected annually, which is about 18 % of all malignant neoplasms [6, 7]. Lacteal cyst cancer (papillary cancer, papillary cystadenocarcinoma) is one of the rarest forms of BRCA, the frequency of which varies from 0.3 to 2.2 % [4, 9]. The most common intracystic cancer occurs at the age of 55 to 60 years [5, 7]. It is characterised by a slow rate of tumor growth and a more positive clinical course in comparison with other forms of BRCA. Because of a small number of studies devoted to the diagnosis of intracystic cancer, and despite the rapid progress of computer technology and the constant emergence of new improved diagnostic methods in mammology, timely detection of the pathology continues to be a relevant issue of clinical oncology [1, 2, 3, 8].

Morphological verification is necessary to diagnose intracystic breast cancer. The main method of obtaining material from the cystic cavity is a fine-needle aspiration biopsy (FNAB). The liquid aspirated from the cystic cavity during FNAB is used for cytological examination of a cyst with papillary growths [4, 5]. In the works of N. V. Zabolotskaya, it is indicated that the aspirate is more informative if it is obtained directly from a solid parietal component, since tumor cells in the liquid contents of the cyst may not be enough to diagnose [5, 10]. However, in case of small sizes of intracystic parietal growths, it can be difficult to obtain material from them even aiming under ultrasound control [5, 8, 11]. Due to the above-stated, we have developed a new improved method of cytological diagnosis of cancer in the breast cyst that allows increasing the informativeness of the FNAB procedure.

The purpose of the study

Creation a new improved method of cytological diagnosis of cancer in a breast cyst.

Materials and methods

We examined 67 women with suspected intracystic breast cancer. All patients underwent a comprehensive examination according to the standard diagnostic algorithm, which included examination and palpation of the mammary glands and areas of regional lymph drainage, ultrasound examination (US) of the mammary glands and axillary areas in B-mode ultrasound, doppler ultrasonography, compression elastography, shear wave elastography, X-ray mammography, FNAB according to traditional and advanced methods under ultrasound control and trepanobiopsy of the a solid parietal component (with a diameter of more than 15 mm). The average age of the patients was 50,19±10,465 years.

A syringe of 20 ml volume and a needle of 22 G diameter were used during FNAB according to the traditional method. Under ultrasound control, after skin preparation with an antiseptic solution has been made, a puncture needle was inserted into the cyst cavity, after which its contents were completely aspirated. The material was sent for cytological examination. In the case of the presence

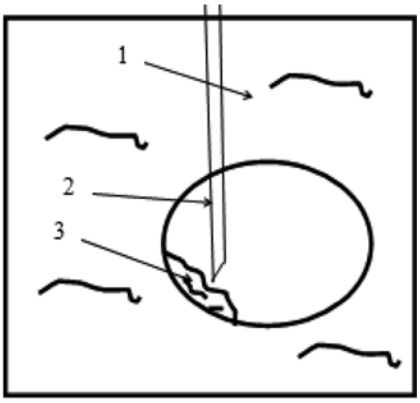

Fig.1. The needle insertion into the cyst cavity with a parietal component, where 1 – mammary gland tissue, 2 – a puncture needle in the cyst cavity, 3 – a parietal solid component.

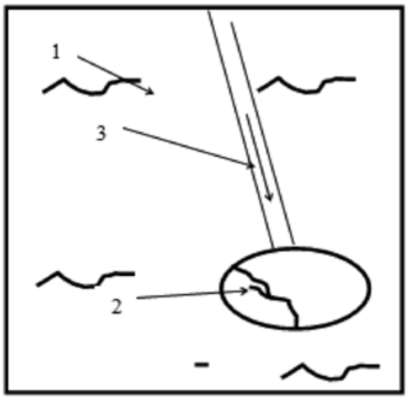

Fig.2. The insertion of an ozone-oxygen mixture into the cyst cavity, where 1- mammary gland tissue, 2 – a parietal intracystic component, 3 – the insertion of an ozone–oxygen mixture through a puncture needle.

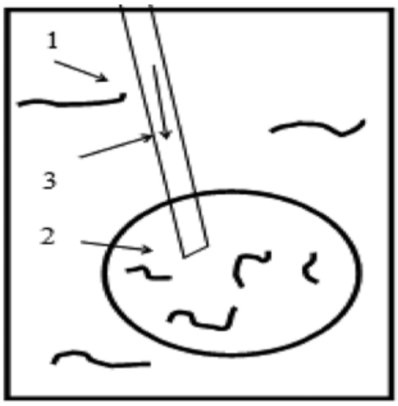

Fig.3. The insertion of an excessive amount of saline solution into the cyst cavity, where 1 – mammary gland tissue, 2 – the contents of the cyst with a fragmented parietal component, 3 – the insertion of saline solution into the cystic cavity.

of parietal growths, the needle was inserted directly into the solid component with subsequent aspiration. Before removing the needle, the plunger of the syringe was released, then it was removed, and the puncture site was pressed with a rolled gauze for 3–5 minutes. Then the contents of the syringe were poured into a test tube and centrifuged, after that a cytological examination was performed.

The traditional technique of FNAB of cysts with a solid parietal component has a number of disadvantages: atypical cells are not always present in the liquid content, puncture of parietal growths is often ineffective, since getting into the area of interest is difficult with its diameter less than 5 mm. As part of the study, false negative results were obtained during cytological examination of a number of patients with intracystic breast cancer (*Fig.1*). The presence of these disadvantages prompted the creation of a new improved FNAB method (Patent RU № 2712055).

The essence of the new diagnostic method is that before aspiration of the contents, ozone is injected into the cystic cavity, which is a strong oxidizer and quickly necrotizes the outer layer of the parietal formation, thereby increasing its fragility and degree of fragmentation, which increases the possibility of detecting atypical cells in the aspirated liquid. The proposed method is carried out in several stages. At the first stage, an ultrasound examination is performed to detect cysts with parietal growths in the mammary gland tissue. Then, under ultrasound control, a puncture is performed with aspiration of at least 50 % of the contents of the cystic cavity, followed by the introduction of an ozone-oxygen mixture at a concentration of 5 micrograms / ml, which gives partial necrosis of the outer layer of the parietal component. The contents of the cyst are removed after 1 minute (*Fig. 1, 2*).

At the second stage, an excessive amount of saline solution in the volume of 150 % of the initial contents of the cystic cavity is injected into the cyst cavity, which leads to the formation of a turbulent fluid flow tearing off the necrotic surface of the parietal component, which increases the probability of detecting unchanged atypical cells in the aspirate (*Fig. 3*).

At the third stage, the entire volume of cyst contents is aspirated and then centrifuged, followed by cytological examination *(Fig. 4*).

To obtain an ozone-oxygen mixture of the desired concentration, the medical ozone therapy machine YOTA-60–01-Medozon was used, which has been recommended for use in medical practice in the Russian Federation since 1996 (registration certificate 29/06050796/1561–01) and is included in the Russian Register of Medical Equipment. YOTA-61–01 is the only medical device recommended by Ministry of Health of the Russian Federation as a material and technical support for ozone therapy (registration certificates of medical technologies FC – 2005/058, FC – 2007/014).

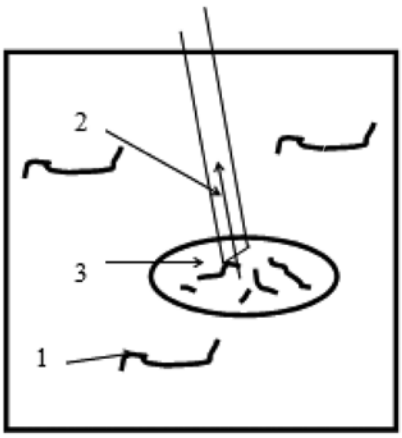

Fig.4. Evacuation of the contents of the cystic cavity with saline solution, where 1 – mammary gland tissue, 2 – the evacuated contents of the cyst, 3 – a reduced cystic cavity with atypical cells detached from the parietal component.

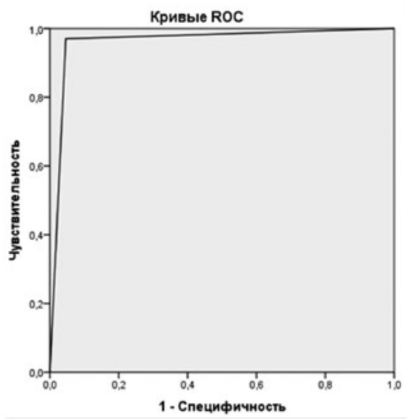

Fig.5. The ROC-analysis in order to study the diagnostic and prognostic value of a new method of diagnosing cancer in a breast cyst.

Results and discussion

The patients were divided into two groups depending on the method of performing FNAB.

FNAB was performed on 33 patients with intracystic breast cancer according to the traditional method under ultrasound control. FNAB was performed on 34 patients according to a new improved technique using the preliminary introduction of an ozone oxygen mixture.

Atypical cells were not detected during cytological examination in 18.2 % (n=6) of patients with intracystic breast cancer who underwent FNAB according to the standard technique, so the study turned out to be false negative, atypical cells were detected in the remaining 81.8 % (n=27) of patients.

During cytological examination of the contents of the cystic cavity, atypical cells were found in 97.06 % (n=33) of patients with intracystic breast cancer who underwent FNAB using a new technique.

Thus, the sensitivity of FNAB according to the traditional method of the diagnosis of intracystic breast cancer was 81.8 %, and the sensitivity of the new improved method was 97.06 %, which indicates the reasonability of using the latter in order to improve the diagnosis of intracystic cancer at the pre-operative stage.

In order to study the diagnostic and prognostic value of a new method of diagnosing cancer in a breast cyst, we carried out the ROC-analysis. A statistically significant correlation was revealed between the detection of atypical cells in the contents of the cystic cavity and the diagnosis of «cancer in the cyst».

The area under the curve was 0.984 (95 % CI – 0.961–0.995), which corresponds to the excellent quality of the classifying ability (*Fig. 5*).

Conclusions

1. The presence of a number of disadvantages of the existing traditional FNAB method limits its use in the diagnosis of intracystic breast cancer, because there is a high probability of obtaining false negative results.
2. A new improved method of diagnosing cancer in a breast cyst using an ozone oxygen mixture has turned out to be more effective than the existing one, which proves the reasonability of using FNAB with an ozone oxygen mixture in order to improve the diagnosis of intracystic cancer at the pre-operative stage (AUROC – 0,984, CI 0,961–0,995).

References

1. *Vasiliev A. Y. Difficulties of differential diagnosis of non-palpable breast formation in outpatient practice / A. Yu. Vasiliev, T. V. Pavlova, O. O. Manuilova [et al.] // Radiology – practice. – 2016. – No. 5. – P. 47–52.*
2. *Vladimirova A. V. The effectiveness of cytological diagnosis of breast cancer metastases in regional lymph nodes / A. V. Vladimirova, V. I. Novik // Questions of oncology. – 2016. – No. 3. – P. 465–469.*
3. *Volchenko N. N. Difficulties of cytological diagnosis of breast diseases based on trepanobiopsies / N. N. Volchenko, O. V. Borisova, A. G. Ermolaeva, V. Yu. Melnikova, A. N. Petrov // Clinical laboratory diagnostics. – 2017. – Vol. 62. – No. 4. – P. 210–215.*
4. *Gazhonova V. E. Screening of breast cancer: the state of the problem and solutions / V. E. Gazhonova, N. N. Vinogradova, A. V. Zubarev // Kremlin medicine. – 2017. – V. 3. – P. 6–11.*
5. *5. Zabolotskaya N. V. Ultrasound diagnosis of breast diseases. Practical guidelines for ultrasound diagnosis / N. V. Zabolotskaya, V. V. Mitkov. – Moscow: Vidar, 2006. – P. 563–609*
6. *Kaprin A. D. Malignant neoplasms in Russia in 2015 (morbidity and mortality). M .: MNIOI them. P. A. Herzen is a branch of the Federal State Budgetary Institution «NMIRC» of the Ministry of Health of Russia. – 2017. – P. 250.*
7. *Semiglazov V. F. Minimal breast cancer (prevention, detection, treatment) / V. F. Semiglazov, A. G. Vesnin, V. M. Moiseenko. – M .: Hippocrates, 2017. – P. 240.*
8. *Zapirova S. B. Ozone therapy is a modern method of conservative treatment of breast cysts // Research and practice in medicine. – 2015. – T. 2. – N 1. – P. 81.*
9. *Atasoy M. M. Vacuum-assisted stereotactic biopsy for isolated BI-RADS 4 microcaltifications: evaluation with histopathology and midterm follow-up results / M. M. Atasoy, N. Tasali, R. Cubuk, B. Narin [et al.] // Diagnostic and Interventional Radiology. – 2015. – V. 21. – N 1. – P. 22–27.*
10. *Chen S. Q., Liu J. E., Zhang Z. X., Li Z. Self-acceptance and associated factors among Chinese women with breast cancer. // Journal of Clinical Nursing. – 2017. – V. 10. – P. 1111–1119.*
11. *Diviani S. N., Kardasis N. D. Analysis of the cytological features supporting the diagnosis of lobular breast cancer. Factors associated with equivocal diagnoses // J Buon. – 2015. – V. 20. – P. 40–44.*

Received 06.06.2022
Revised 18.06.2022
Accepted 27.06.2022

INFORMATION ABOUT AUTHORS

Arabachyan Mariam Ilichovna, *Oncologist, ultrasound diagnostics doctor, junior scientist of the Problem Research Laboratory «Diagnostic investigations and minimally invasive technologies», Smolensk State Medical University, Ministry of Health of Russia Smolensk, Russian Federation.
ORCID: https://orcid.org/0000-0002-0919-2083, Tel. +79101169208, e-mail: arabachyanmariam@mail.ru*

Borsukov Alexey Vasilyevich, *MD, Professor, Head of the Problem Research Laboratory «Diagnostic investigations and minimally invasive technologies», Smolensk State Medical University, Ministry of Health of Russia Smolensk, Russian Federation.
ORCID: https://orcid.org/0000-0003-4047-7252, Tel. +79036492210, e-mail: bor55@yandex.ru*

DOI:10.33667/2782-4101-2022-2-12-16

NOVEL METHOD FOR QUANTIFYING HEPATIC STEATOSIS IN PATIENTS WITH METABOLICALLY ASSOCIATED FATTY LIVER DISEASE

Alexey Borsukov, Daria Venidiktova, Semen Borsukov

Fundamental research laboratory "Diagnostic researches and minimally invasive technologies" of Smolensk State Medical University, the Ministry of Health of the Russian Federation, Smolensk, Russia

SUMMARY

Introduction. *The article presents an overview of novel complex algorithm based on methods of ultrasound steatometry, combined elastography and dual-energy X-ray absorbtiometry in "Whole body" mode in diagnostic and monitoring of metabolically associated fatty liver disease.*

The purpose of the study: *to assess the possibility of quantitative ultrasound steatometry using in the detection and monitoring of metabolically associated fatty liver disease.*

Material and methods. *157 patients were examined. The main group consisted of 47 patients with liver steatosis; 45 patients with steatohepatitis and clinically insignificant liver fibrosis (F0-F1); 32 patients with steatohepatitis and clinically significant liver fibrosis (F2-F3); 33 patients with focal hepatic steatosis. We used complex algorithm based on methods of questionnaires, laboratory tests, ultrasound steatometry, combined elastography and dual-energy x-ray absorbtiometry in "Whole body" mode, liver biopsy. to determine the severity of steatosis, a scale was used: S0 – no steatosis; <2.19 dB/cm; S1, minimal steatosis, <5% of hepatocytes with steatosis; 2.2–2.29 dB/cm; S2 – moderate steatosis, <6–32% of hepatocytes with steatosis; 2.3–2.9 dB/cm; S3 – severe steatosis, <33–100% of hepatocytes with steatosis; >2.9 dB/cm.*

Results and conclusion. *It is possible to use quantitative ultrasound steatometry for metabolically associated fatty liver disease, as a reference method both for the initial detection of the disease and for monitoring non-drug treatment (sensitivity 90.7%, specificity 92.4%). The optimal complex for the diagnosis and monitoring of non-drug treatment of metabolically associated fatty liver disease includes an assessment of the level of compliance, the use of quantitative ultrasound steatometry and dual-energy X-ray absorptiometry in the «Whole body» mode (sensitivity 92.8%, specificity 92.3%).*

KEYWORDS: *metabolically associated fatty liver disease, ultrasound steatometry, liver biopsy, dual-energy X-ray absorbtiometry.*

CONFLICT of INTEREST. *The authors declare no conflict of interest.*
Funding. *Funding for the study was carried out from the personal funds of the authors.*

Introduction

Currently, the term non-alcoholic fatty liver disease (NAFLD) is understood as an independent nosological unit, the pathogenesis of which is based on the phenomena of insulin resistance and hyperinsulinemia and which includes a spectrum of clinical and morphological changes in the liver parenchyma: hepatic steatosis, steatohepatitis, hepatic fibrosis, hepatic cirrhosis and its complications (including hepatocellular carcinoma) [1]. In 2020, a new adaptive concept was proposed – MAFLD (Metabolically Associated Fatty Liver Disease), which allows emphasizing the systemic and multifactorial nature of the pathogenesis of a unified lesion of the hepatic parenchyma and personalizing the volumes and directions of treatment and diagnostic care in various clinical variants of the disease [2].

In different countries, the incidence of MAFLD varies and averages 6.3–33%, reaching a level of 62–93% in obese patients [2]. In most countries of the world, MAFLD ranks first among liver diseases [3]. These data correspond to the prevalence of the metabolic syndrome and its components [4, 5, 6].

The prognosis of the disease and management tactics are determined primarily by the severity of liver steatosis [7–10], which further affects the timing of the progression of the underlying disease and determines the risk of complications [11–13].

The problem of diagnosing MAFLD remains quite relevant at the present stage of medicine, as well as further treatment and monitoring [14–16]. Consequently, the problem is complex, and therefore requires a meaningful algorithm for early diagnosis [17, 18]. The importance of an adequate and timely assessment of the severity of the pathological process in the liver is beyond doubt: it is necessary in clinical practice to determine the stage, prognosis of the disease and the ability to timely adjust the tactics of treating patients [19, 20]. The use of modern instrumental methods has significantly expanded the amount of information received on the detection rate, periods of early development of liver diseases [21–23].

Ultrasound steatometry is in special, yet little-studied niche in gastroenterology and ultrasound diagnostics, which confirms the growing interest and participation of specialists in various scientific forums dedicated to the possibilities of methods for detecting and assessing MAFLD [24–26]. A general methodological view on the role and place of ultrasonic steatometry in a multidisciplinary hospital has not yet been developed [27, 28].

As MAFLD progresses, the process of pathological changes proceeds sequentially through several stages: from steatosis, stromal inflammatory reaction, stepwise necrosis to the development of fibrosis and, in the terminal stage, liver cirrhosis with the possibility of neoplasia in the form of hepatocellular carcinoma [29, 30]. It is known that the assessment of the severity of liver steatosis is important for determining the stage of non-alcoholic fatty liver disease and further prognosis [31].

A reliable method for diagnosing liver pathology is morphological verification, i.e. liver biopsy [32]. Unfortunately, this method is associated with many complications and technical difficulties, so the search for highly informative methods for early, non-invasive diagnosis of liver pathology is constantly being carried out [33]. One of these methods, which allows to assess the severity of liver steatosis, is ultrasound steatometry. This method is based on a quantitative assessment of the attenuation coefficient of an ultrasound wave in tissues in dB/cm (or dB/cm/MHz) and has a number of advantages, such as the possibility of an informative assessment of diffuse and focal changes in the liver in real time, good patient tolerance, no complications, cost-effectiveness [34]. Currently, there is a limited number of works on the use of ultrasound quantitative steatometry in non-alcoholic fatty liver disease, despite the fact that this diagnostic method is promising due to the possibility of non-invasively, repeatedly and quantitatively assessing liver steatosis.

Purpose of the study: to assess the possibility of quantitative ultrasound steatometry using in the detection and monitoring of metabolically associated fatty liver disease.

Material and methods

157 people with metabolically associated fatty liver disease were examined based on the Fundamental Research Laboratory «Diagnostic research and minimally invasive technologies». The main group consisted of 47 patients with liver steatosis (MAFLD); 45 patients with steatohepatitis (MASH) and clinically insignificant liver fibrosis (LF) (F0-F1); 32 patients with steatohepatitis and clinically significant LF (F2-F3); 33 patients with focal hepatic steatosis (FLS). Data on the distribution of patients by sex and age are presented in *Table 1*.

Control group 1 (n=102) – patients with a normal level of adipose tissue in the body according to non-invasive bioimpedancemetry, and not suffering from damage to the liver tissue according to clinical, laboratory and instrumental research methods.

Control group 2 (n=44) – patients with MAFLD, who underwent the entire complex of clinical, laboratory and instrumental procedures used in this study, without including ultrasound quantitative steatometry.

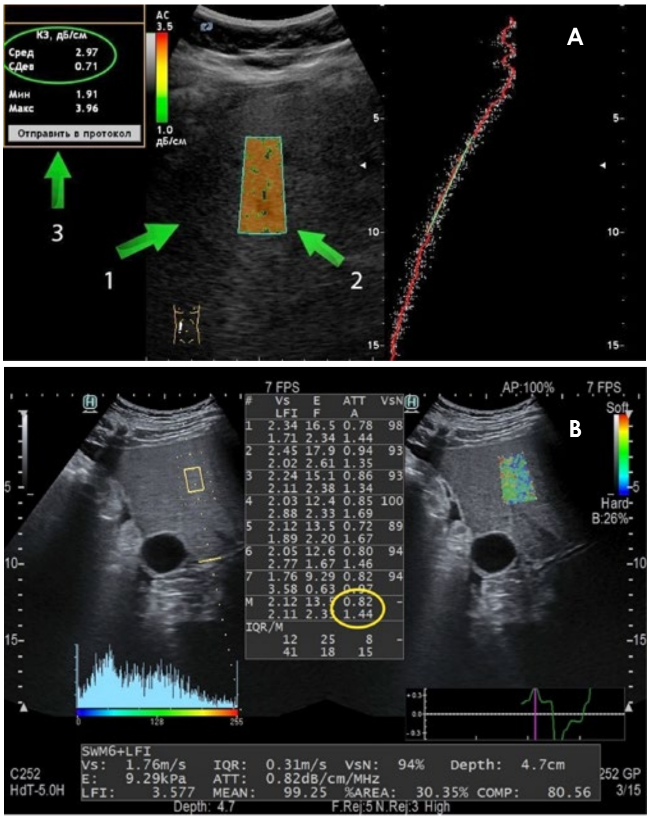

Fig. 1. A. Window of results of ultrasound steatometry: 1 – liver, 2 – active zone of measurement, 3 – short-circuit indicator of the ultrasound wave. B. Window of results of combined elastography: 1 – liver, 2 – active zone of measurement of short-circuit ultrasound wave, 3 – indicator of short-circuit ultrasound wave, quantitative indicator of inflammatory activity (A-index), quantitative indicator of the severity of liver fibrosis (F-index).

The study of patients of the main group (n=157) included:

- Stage 1 – questionnaires (SF-36 V.2., CAGE, AUDIT, DEBQ, CLDQ-NAFLD, IPAQ)
- Stage 2 – clinical and biochemical blood tests (including coagulogram and lipidogram), general urinalysis.
- Stage 3 – liver ultrasound with a quantitative assessment of the ultrasound wave attenuation coefficient (dB/cm), combined elastography of the liver with a quantitative assessment of liver steatosis, activity of the inflammatory process, severity of LF. to determine the severity of steatosis, a scale was used: S 0 – no steatosis; <2.19 dB/cm; S 1, minimal steatosis, <5 % of hepatocytes with steatosis; 2.2–2.29 dB/cm; S 2 – moderate steatosis, <6–32 % of hepatocytes with steatosis; 2.3–2.9 dB/cm; S 3 – severe steatosis, <33–100 % of hepatocytes with steatosis; >2.9 dB/cm.

The window of results and the main indicators evaluated during quantitative ultrasound steatometry are shown in *Fig. 1.*

Table 1
Distribution of patients by age and sex

Groups	Total		Men		Women		Average age, year
	n	%	n	%	n	%	
1 gr. MAFLD (n=47)	47	29,9	24	15,3	23	14,6	34,69±1,97
2 gr. MASH with clinically insignificant LF (F0-F1) (n=45)	45	28,7	24	15,3	21	13,4	51,42±1,42
3 gr. MASH with clinically significant LF (F2-F3) (n=32)	32	20,4	18	11,5	14	8,9	49,34±1,91
4 gr. FLS (n=33)	33	21,0	17	10,8	16	10,2	43±2,64
Total (n=157)	157	100	83	52,9	74	47,1	44,62±1,07

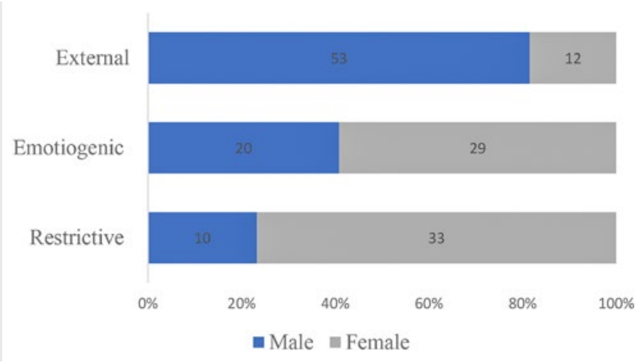

Fig. 2. Distribution of patients according type of eating disorder (DEBQ).

- Stage 4 – determination of complex indices: fatty liver index (FLI), assessment of the state of the liver according to the fibrosis scale in NAFLD (NFS), fibrosis index-4 (FIB-4).
- Stage 5 – dual-energy X-ray absorbtiometry (DXA) in “Whole body” mode.
- Stage 6 – trepan-biopsy of the liver with ultrasound control, with the study of micropreparations on the SAF scale (n=49 (32,7 %).

Non-drug measures in all patients were taken according to the general principles of weight loss with its subsequent maintenance: teaching patients a proper lifestyle with a change in eating habits (with the participation of a general practitioner); hypocaloric diet; keeping a food diary; physical exercises.

Statistical processing of the research results was carried out in the Microsoft Excel 2017 database. Data analysis was carried out using descriptive statistics and comparison of samples (using parametric and nonparametric criteria). Pearson rank correlation analysis was used to assess the relationship between two variables. Coefficient r greater than 0 at $p \leq 0.05$ was taken as reliable. Indicators of predictive value (sensitivity and specificity) were determined.

Results

The results of the interpretation of the SF-36 questionnaire at the first visit of patients to the research center showed the results of quality of life slightly below the average levels in the general population of the Russian population. All patients of the control group 1 showed results above the average levels (minimum values for the physical component of health – 79, for the psychological component of health – 72).

The CLDQ-NAFLD (Chronic Liver Disease Questionnaire – Non-Alcoholic Fatty Liver Disease) questionnaire assess the level of quality of life in patients with chronic liver diseases (in particular, NAFLD) on 6 factors: fatigue, anxiety, emotional function, abdominal symptoms, systemic symptoms, activity. Patients of all studied groups assess their physical and psychological state above the average value; high results are noted in groups 1 and 4, which is probably due to the absence of clinical manifestations of NAFLD in most representatives of this group of patients.

The distribution of patients in the main study groups according to the results of DEBQ questionnaire is presented in *Fig. 2*.

In groups of patients 1 and 4, no increase in liver enzymes was recorded. In groups 2 and 3, there was an increase in the level of hepatic transaminases with a predominance of ALT. Additionally, in group 3, there were also changes in the direction of growth of ALT, AST, alkaline phosphatase, total and direct bilirubin.

In patients 1, 2 and 4 of the main study groups, there were no deviations of the coagulogram parameters from normal values. In the majority of patients of the 3rd main study group, at the recruitment stage, a decrease in blood clotting ability (prolongation of prothrombin time) was revealed.

Glucose levels differed significantly in groups 1–4 due to the presence in each of the groups of patients with type 2 diabetes.

In the majority of patients of the main study groups (except for patients of groups 1 and 4), the lipid profile showed a decrease in HDL levels, an increase in TG and LDL. Some of them also had an increase in total cholesterol levels. Increased levels of total cholesterol and LDL have been considered as risk factors for diabetes mellitus and atherosclerosis. a slight increase in triglyceride levels was also detected in patients with type 2 diabetes.

The distribution of patients in the main study groups according to the results of quantitative ultrasound steatometry is presented in *Table 2*.

The coincidence of the data of liver ultrasound quantitative steatometry with the data of combined elastography with the determination of liver steatosis at degrees of liver steatosis S 0 and S 3 was revealed, in the intermediate intervals S 1-S 2 there was a discrepancy in the data per 1 patient in each of the groups. In this group of patients, there was a complete agreement between the data ob-

Table 2

Distribution of patients in the main study groups (n=157) according to the results of quantitative ultrasound steatometry

Liver steatosis (grade)	1 gr. (n=47)		2 gr. (n=45)		3 gr. (n=32)		4 gr.* (n=33)		Total (n=157)	
	n	%	n	%	n	%	n	%	n	%
S 1	27	57,45	18	40	13	40,62	19	57,58	77	49
S 2	13	27,66	16	35,56	10	31,25	13	39,39	52	33,1
S 3	7	14,89	11	24,44	9	28,13	1	3,03	28	17,8

** In group 4 quantitative ultrasound steatometry was performed in a preselected area of interest (in the focus of focal liver steatosis).*

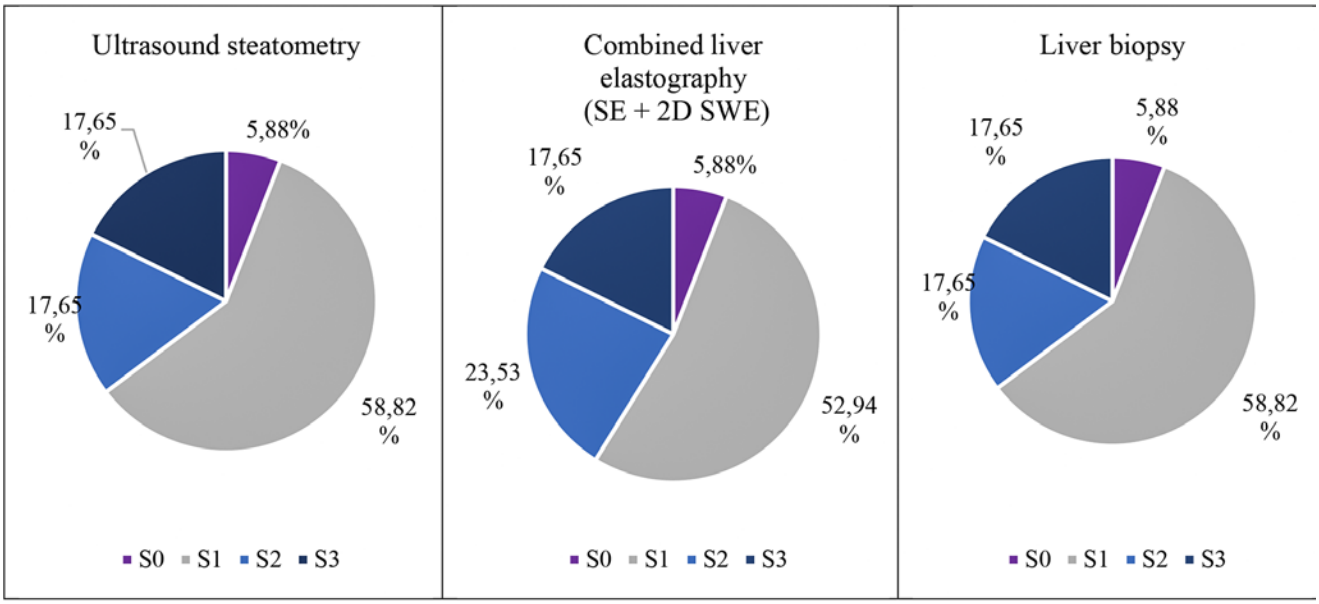

Fig. 3. The ratio of indicators of liver ultrasound steatometry with the determination of the attenuation coefficient of the ultrasound wave (dB/cm), combined elastography with the determination of liver steatosis (dB/cm/MHz) and histological examination of liver biopsy specimens according to the SAF scale in patients (n=17) who agreed to re-biopsy 36 months after the start of the study.

Table 3

Dynamics of changes in the severity of liver steatosis according to the histological examination of liver biopsy specimens (SAF scale) in patients of the main study groups 1–3

	Proportion of patients (%) who agreed to a liver biopsy at baseline (n=49)	Proportion of patients (%) who agreed to a liver biopsy at baseline (n=17)*	Proportion of patients (%) who agreed to a liver biopsy at the end of the study (n=17)
		Liver steatosis	
S0	2,04	0	5,88
S1	32,65	29,41	58,82
S2	38,78	41,18	17,65
S3	26,53	29,41	17,65
		Activity of the inflammatory process	
A0	32,65	23,53	52,94
A1	14,29	17,65	23,53
A2	24,49	29,41	17,65
A3	16,33	23,53	5,88
A4	12,24	5,88	0
		Liver fibrosis	
F0	38,78	35,29	64,71
F1	20,41	23,53	5,88
F2	14,29	23,53	11,76
F3	14,29	11,76	11,76

**The same patients who consented to repeat liver biopsy at the end of the study.*

tained using ultrasound steatometry of the liver with the data obtained from the histological examination of biopsy specimens (*Fig. 3*).

The distribution of the results of liver biopsy of patients who consented to repeat biopsy according to the severity of steatosis (S0-S3), the activity of the inflammatory process (A0-A4) and fibrosis (F0-F3) are presented in *Table 3*.

Based on the results of the primary DXA study, the results shown in *Table 4* were obtained.

Table 4

Distribution of patients of the main group based on the fat mass index according to DXA data in the «Whole Body» mode

Fat mass index	1 gr. (n=47)		2 gr. (n=45)		3 gr. (n=32)		4 gr. (n=33)	
	n	%	n	%	n	%	n	%
Excess	13	27,66	13	28,89	8	25	19	57,58
Obesity 1 grade	16	34,04	18	40	9	28,13	12	36,36
Obesity 2 grade	14	29,79	13	28,89	14	43,75	2	6,06
Obesity 3 grade	4	8,51	1	2,22	1	3,12	0	0

Conclusions

1. It is possible to use quantitative ultrasound steatometry for metabolically associated fatty liver disease, as a reference method both for the initial detection of the disease and for monitoring non-drug treatment (sensitivity 90.7%, specificity 92.4%).
2. The optimal complex for the diagnosis and monitoring of non-drug treatment of metabolically associated fatty liver disease includes an assessment of the level of compliance, the use of quantitative ultrasound steatometry and dual-energy X-ray absorptiometry in the «Whole body» mode (sensitivity 92.8%, specificity 92.3%).

References

1. *Ivashkin VT, Maevskaya MV, Pavlov CS, et al. Clinical guidelines for the diagnosis and treatment of non-alcoholic fatty liver disease of the Russian Society for the Study of the Liver and the Russian Gastroenterological Association. Russian Journal of Gastroenterology, Hepatology, Coloproctology.– 2016.– T. 26.– No. 2.– P. 24–42. (In Russ.).*
2. *Lazebnik LB, Golovanova EV, Turkina SV, et al. Non-alcoholic fatty liver disease in adults: clinic, diagnosis, treatment. Recommendations for therapists, third edition. Experimental and clinical gastroenterology. 2021; 185(1): 4–52. DOI: 10.31146/1682–8658-ecg-185–1–4–52 (In Russ.).*
3. *Zhou, J. Epidemiological Features of NAFLD From1999 to 2018 in China / J. Zhou // Hepatology.– 2020.– V. 71.– No. 5.– P. 1851–1864.*

4. O'Neill, S. Metabolic syndrome: a closer look at the growing epidemic and its associated pathologies / S. O'Neill, L. O'Driscoll // Obesity reviews.– 2015.– V. 16.– No. 1.– P. 1–12.
5. Sheveleva MA, Hudyakova NV, Shishkin AN, et al. Non-alcoholic fatty liver disease and metabolic syndrome. Health is the basis of human potential: problems and ways to solve them.– 2019.– T. 14.– No. 2.– P. 632–642. (In Russ.).
6. Godoy-Matos, A. F. NAFLD as a continuum: from obesity to metabolic syndrome and diabetes / A.F. Godoy-Matos, W. S.S. Júnior, C.M. Valerio // Diabetology & Metabolic Syndrome.– 2020.– V. 12.– No. 1.– P. 1–20.
7. DamLarsen, S. Long – term prognosis of fatty liver: risk of chronic liver disease and death / S. DamLarsen, M. Franzmann, V. Andersen // Gut.– 2004.– V. 53, No. 7 – P. 750–755.
8. EASL-ALEH Clinical Practice Guidelines: Noninvasive tests for evaluation of liver disease severity and prognosis // Journal of Hepatology.– 2015.– V. 63 – No. 1.– P. 237–264.
9. McPherson, S. Evidence of NAFLD progression from steatosis to fibrosingsteatohepatitis using paired biopsies: implications for prognosis and clinical management / S. McPherson, T. Hardy, E. Henderson et al. / Journal of Hepatology.– 2015 – V. 62.– P. 1148–1155.
10. Yakovenko MS. Correction of the metabolic syndrome in patients with non-alcoholic fatty liver disease and eating disorders. Attending doctor.– 2020.– No. 2.– P. 23–27. (In Russ.).
11. Dedov II, Melnichenko GA, Shestakova MV, et al. National clinical guidelines for the treatment of morbid obesity in adults. 3rd revision (treatment of morbid obesity in adults). Obesity and metabolism.– 2018.– T. 15.– No. 1.– P. 53–70. (In Russ.).
12. Ahmedov VA. Non-alcoholic fatty liver disease is a dramatic consequence of obesity. Medical alphabet.– 2019.– T. 3.– No. 20.– P. 37–40. (In Russ.).
13. Shelihovskaya PA, Sabirova AI, Mamytova AB, et al. Nephrotic and cerebrovascular risks in non-alcoholic fatty liver disease. The Scientific Heritage.– 2020.– No. 46–3 (46).– P. 71–76. (In Russ.).
14. Kashenko VA, Micinskaya AI, Sokolov AY, et al. Obesity and non-alcoholic fatty liver disease: therapeutic options. Siberian Medical Review.– 2020.– No. 3 (123).– P. 20–29. (In Russ.).
15. Venidiktova DY. The level of patient compliance as the basis for the appointment of personalized non-drug treatment of non-alcoholic fatty liver disease. Practical medicine.– 2021.– T. 19.– No. 1.– P. 96–105. (In Russ.).
16. Zvenigorodskaya LA, Mkrtumyan AM, Shinkin MV, et al. Clinical significance of key components of the adipo-cardiovascular axis in patients with type 2 diabetes mellitus and non-alcoholic fatty liver disease. effective pharmacotherapy.– 2021.– T. 17.– No. 20.– P. 26–36. (In Russ.).
17. Borsukov AV, Venidiktova DY. Evaluation of the comparative effectiveness of methods for instrumental diagnosis of liver steatosis in patients with metabolic syndrome. Practical medicine.– 2018.– T. 16.– No. 2.– P. 16–21. (In Russ.).
18. Zhirkov II, Gordienko AV, Pavlovich IM, et al. Non-invasive diagnostic methods for steatosis in non-alcoholic fatty liver disease. Experimental and clinical gastroenterology.– 2020.– T. 174.– No. 5.– P. 61–66. (In Russ.).
19. Trofimchuk TA, Fedorova TE, Efimenko NV, Muhotin NA. Modern aspects of etiopathogenesis and treatment of non-alcoholic fatty liver disease. Spa medicine.– 2017.– No. 3.– P. 107–115. (In Russ.).
20. Venidiktova DY, Borsukov AV. Ultrasound quantitative liver steatometry in patients with overweight fat: the possibilities of an improved technique. Radiation diagnostics and therapy.– 2020.– T. 11.– No. 1.– P. 64–69. (In Russ.).
21. Pavlov ChS, Kotovich MM. The place of biopsy and morphological examination of liver tissue in children and adults in the clinician's practice. Clinical medicine.– 2007.– T. 85.– No. 9.– P. 72–77. (In Russ.).
22. Maevskaya MV, Ivashkin VT. Liver and nutrition. Optimal diet for non-alcoholic fatty liver disease. Russian journal of gastroenterology, hepatology, coloproctology.– 2018.– T. 28.– No. 5.– P. 105–116. (In Russ.).
23. Tarasova LV, et al. Review of laboratory diagnostic methods used in non-alcoholic fatty liver disease (NAFLD) and alcoholic liver disease (ALD) at the present stage. Experimental and clinical gastroenterology.– 2019.– No. 4 (164).– P. 72–77. (In Russ.).
24. Bakulin IG, Sandler UG, Keyan VA, et al. Assessment of liver steatosis using a non-invasive method: myth or reality? Doctor. RU.– 2015.– No. 12.– P. 57–64. (In Russ.).
25. Karlas, T. Non-invasive assessment of hepatic steatosis in patients with NAFLD using controlled attenuation parameter and 1 H-MR spectroscopy / T. Karlas // PloS one.– 2014.– V. 9.– № 3.– P. 91–98.
26. Pu, K. Diagnostic accuracy of controlled attenuation parameter (CAP) as a non-invasive test for steatosis in suspected non-alcoholic fatty liver disease: a systematic review and meta-analysis / K. Pu // BMC gastroenterology.– 2019.– V. 19.– № 1.– P. 1–11.
27. Cosgrove, D. EFSUMB Guidelines and Recommendations on the Clinical Use of Ultrasound Elastography. Part 2. Applications / D. Cosgrove, J. Bamber, C.F. Dietrich et al. // Ultrashal Med.– 2013 – P. 238–253.
28. Borsukov AV, Morozova TG. Complex elastography in the differential diagnosis of diffuse liver diseases. Scientific notes of the Oryol State University.– 2015.– No. 4.– P. 378–383. (In Russ.).
29. Bedossa, P. Current histological classification of NAFLD: strength and limitations / P. Bedossa // Hepatology International.– 2013.– V. 7.– № 2.– P. 765–770.
30. Byrne, C.D. What's new in NAFLD pathogenesis, biomarkers and treatment? / C.D. Byrne, G. Targher // Nature reviews gastroenterology & hepatology.– 2020.– V. 17.– № 2.– P. 70–71.
31. Barigou M. New trends in non-alcoholic fatty liver diseases (NAFLD) / M. Barigou, L. Favre, M. Fraga, F. Artru // Revue medicale suisse.– 2020.– V. 16.– № 687.– P. 586–591.
32. Gerhardt, F. Biopsy rate and nonalcoholic steatohepatitis (NASH) in patients with nonalcoholic fatty liver disease (NAFLD) / F. Gerhardt // Scandinavian Journal of Gastroenterology.– 2020.– P. 1–6.
33. Falck-Ytter, Y. The risks of percutaneous liver biopsy / Y. Falck-Ytter, A.J. McCullough, J.F. Cadranel et al. // Journal of Hepatology.– 2001.– V. 33.– № 1.– P. 764–764.
34. Venidiktova DY, Borsukov AV, et al. Ultrasound steatometry technique for non-alcoholic fatty liver disease: pilot results. Clinical practice.– 2019.– T. 10.– No. 1.– P. 23–29. (In Russ.).

Received 26.06.2022
Revised 18.07.2022
Accepted 24.07.2022

INFORMATION ABOUT AUTHORS

Borsukov Alexey Vasilyevich*, MD, Professor, the Head of Fundamental research laboratory "Diagnostic researches and minimally invasive technologies", Smolensk State Medical University, the Ministry of Health of the Russian Federation, 214019, Smolensk, 28 Krupskoy str., ORCID: 0000-0003-4047-7252. Tel. +79036492210; e-mail: bor55@yandex.ru*

Venidiktova Daria Yuryevna*, Junior scientist of Fundamental research laboratory "Diagnostic researches and minimally invasive technologies", Smolensk State Medical University, the Ministry of Health of the Russian Federation, 214019, Smolensk, 28 Krupskoy str., ORCID: 0000-0001-5497-1476. Tel. +79107850371; e-mail: 92darv@gmail.com*

Borsukov Semen Alekseevich*, the 5-th grade student of Smolensk State Medical University, the Ministry of Health of the Russian Federation, 214019, Smolensk, 28 Krupskoy str., ORCID: 0000-0002-5747-6048. Tel. +79056953120; e-mail: semen.borsukov99@gmail.com*

DOI:10.33667/2782-4101-2022-2-17-21

RESULTS of MORPHOLOGICAL ANALYSIS of ANIMAL HARD TISSUES IN NORMAL AND SIMULATED OSTEOPOROSIS USING A NON–INVASIVE COMPUTED MICROTOMOGRAPHY TECHNIQUE

Alexander Dolgalev[1], Igor Rzhepakovsky[2], Aslan Danaev[1], Vazgen Avanisyan[1], Galina Shulga[1], Artemy Korobkeev[1]

[1]Stavropol State Medical University of the Ministry of Health of the Russian Federation, Stavropol, Russian Federation
[2]North-Caucasus Federal University of the Ministry of Science and Higher Education of the Russian Federation, Stavropol, Russian Federation

SUMMARY

Introduction. *X-ray microtomography is a non-destructive method of microstructural analysis, which has a high level of detail and allows the possibility of assessing the internal architecture of organs and tissues using 3D-analysis[1]. The specifics of working with such equipment can be divided into in vivo and in vitro, i.e. working with live laboratory animals (mice, rats, rabbits) under anesthesia or studying organs and tissues separated from the animal [2].*

The aim of the work *was to study the microstructure of sheep bone tissues in normal and simulated osteoporosis using computed microtomography.*

Materials and methods. *We performed microCT analysis of different sheep bones in normal and experimental osteoporosis. Bone tissue of the jaw, iliac and femur, and teeth were collected from control and experimental animals. Bone tissue samples were fixed in 10% buffered formalin. X-ray microCT scanner Skyscan 1176 (Bruker-microCT, Belgium) and software Skyscan 1176 control program (10.0.0.0), Nrecon (1.7.4.2), DataViewer (1.5.6.2), CT-analyser (1.18.4.0), CTvox (3.3.0r1403) were used to scan and process materials.*

Results. *MicroCT examination and 3D-imaging confirmed the elimination of trabeculae in the metaphyseal region of the femur in sheep with experimental osteoporosis from the centre to the periphery; in addition, 3D-analysis showed a 15.1% decrease in bone percentage, a 7.8% decrease in bone mineral density, and an increase in Tb. Sp. (trabecular separation), Tb. Pf. (trabecular pattern factor) and SMI (structure model index) by 30.2%, 20.8% and 23.6%, respectively, and a decrease in Tb.N. (trabecular number) index by 18.6%, indicating calcium washout, decreased trabecular connectivity and a transition from a lamellar to a rod-like architecture. Similar changes were found in the 3D-analysis of the jaw bone tissue. Thus, a decrease of 18.9% in mineral density was found, as well as a significant increase of 11.58 and 2.21 in the indices, particularly Tb. Pf. and SMI. 3D-analysis of iliac microtomography also indicates a simulation of osteoporosis, as evidenced by a significant increase in the main indices characterising the development of this pathology.*

Conclusions. *The obtained results not only objectively testify to the development of osteoporosis in the experimental animals, but also indicate signs of the adaptation-compensatory reactions of the body, characterized by appearance of large single trabeculae in the metaphysis of the femur as well as by not expressed reduction of bone mineral density and bone tissue area.*

KEYWORDS: *microtomography; nondestructive testing; imaging; bone tissue; osteoporosis; medicine.*

CONFLICT of INTEREST. *The authors declare no conflicts of interest.*

Introduction

Osteoporosis is a progressive metabolic disease of the skeleton, in which there is a generalised reduction of bone mass and bone structure that differs from the age and sex norm, leading to a decrease in physical bone strength and the risk of fractures even with minor trauma. Bone strength is determined by a combination of quantitative and qualitative characteristics: bone mineral density and architectonics, bone metabolism, damage accumulation, and tissue mineralisation. Computed microtomography provides accurate quantitative data on these characteristics without compromising the integrity of the samples under study. [3]

Microtomography is one of the main methods of non-destructive analysis and one of the most common methods of microscopy [1], which visualises the very fine internal structure of objects to provide high-resolution volumetric data at the micron level. This enables the study of microstructures, the precise determination of geometry [4–7], eventually defects and differences in density and morphology. It does not require sample preparation, staining and slicing; settings and parameters have been extensively studied for specific structures [8]. It has great potential for biomedical and bioengineering applications [9]. MicroCT systems are present as laboratory instruments in major laboratories and companies for various types of research and applications including educational purposes [10,11]. Analyses carried out using microtomography can also be useful in terms of compliance with international standards, regulations and in forensic practice [12, 13]. Microtomography analyses can influence the material validation process and quality assessment of finished devices.

Dentistry and Oral and Maxillofacial Surgery (O&M) represent two sectors that influence the biomedical engineering context and where microtomography is widely used because of the need for detailed information on small and complex objects, mineralised structures and with varying densities. The market is characterised by innovative materials and solutions requiring advanced technology in the routine activities of dental laboratories and clinics, such as microtomography [14,15], whose capabilities prove indispensable.

The aim of the work was to study the microstructure of sheep bone tissue in normal and simulated osteoporosis using computed microtomography.

Materials and methods

Bone tissue samples fixed in 10% buffered formalin in accordance with the rules for pathomorphological and histological studies were the objects of study [2].

The samples presented:

Sample № 1

Bone tissue of sheep's jaw in the normal state.

Sample № 2

Bone tissue of sheep's jaw in osteoporosis simulation

Sample № 3

Sheep's tooth in the normal state.

Sample № 4

Osteoporosis simulation in a sheep's tooth

Sample № 5

Sheep femur in the normal state

Sample № 6

Sheep femur in osteoporosis modeling

Sample № 7

Sheep ileum in the normal state

Sample № 8

Sheep ileum in osteoporosis simulation

To study the structure of sheep bones and determine their bone mineral density (BMD), a Skyscan 1176 (Bruker) X-ray computer microCT scanner was used [16]. The system allows creating 3D-reconstructions of objects with resolution up to 9 microns, making it possible to study the structure and density of the examined object without damaging its integrity.

Each bone was scanned along with two phantoms (0.25 and 0.75 g/cm3 calcium hydroxyapatite $Ca5(PO4)3(OH)$) with the diameter corresponding to the thickness of the examined samples.

Scanning parameters in the Skyscan 1176 control program (10.0.0.0, Bruker-microCT, Belgium):

Sample № 1

X-ray voltage 80 kV, X-ray current 300 µA, filter Cu+Al, image pixel size 8,87 µm, tomographic rotation 180º, rotation step 0,3, frame averaging 4.

Sample № 2

X-ray voltage 65 kV, X-ray current 380 µA, filter 0,5 mm Al, image pixel size 8,87 µm, tomographic rotation 180º, rotation step 0,3, frame averaging 4.

Sample № 3

X-ray voltage 90 kV, X-ray current 270 µA, filter Cu 0,1 mm, image pixel size 8,87 µm, tomographic rotation 180º, rotation step 0,3, frame averaging 3.

Sample № 4

X-ray voltage 90 kV, X-ray current 270 µA, filter Cu 0,1 mm, image pixel size 8,87 µm, tomographic rotation 180º, rotation step 0,3, frame averaging 3.

Sample № 5

X-ray voltage 90 kV, X-ray current 259 µA, filter Cu 0,1 mm, image pixel size 35,47 µm, tomographic rotation 180º, rotation step 0,6, frame averaging 4.

Sample № 6

X-ray voltage 90 kV, X-ray current 259 µA, filter Cu 0,1 mm, image pixel size 35,47 µm, tomographic rotation 180º, rotation step 0,6, frame averaging 4.

Sample № 7

X-ray voltage 80 kV, X-ray current 291 µA, filter filter Cu+Al, image pixel size 35,47 µm, tomographic rotation 180º, rotation step 0,3, frame averaging 4.

Sample № 8

X-ray voltage 80 kV, X-ray current 291 µA, filter filter Cu+Al, image pixel size 35,47 µm, tomographic rotation 180º, rotation step 0,3, frame averaging 4.

The scanned objects were reconstructed in Nrecon (1.7.4.2, Bruker-microCT, Belgium) with the following basic reconstruction parameters:

Sample № 1

smoothing 2, ring reduction 10, beam hardening 41, minimum for CS to Image Conversion=0,002, maximum for CS to Image Conversion=0,04.

Sample № 2

smoothing 2, ring reduction 10, beam hardening 41, minimum for CS to Image Conversion=0.002, maximum for CS to Image Conversion=0,08.

Sample № 3

smoothing 4, ring reduction 20, beam hardening 41, minimum for CS to Image Conversion=0.002, maximum for CS to Image Conversion=0,038.

Sample № 4

smoothing 4, ring reduction 20, beam hardening 41, minimum for CS to Image Conversion=0.002, maximum for CS to Image Conversion=0,038.

Sample № 5

smoothing 2, ring reduction 20, beam hardening 41, minimum for CS to Image Conversion=0,002, maximum for CS to Image Conversion=0,03.

Sample № 6

smoothing 2, ring reduction 20, beam hardening 41, minimum for CS to Image Conversion=0,002, maximum for CS to Image Conversion=0,03.

Sample № 7

smoothing 2, ring reduction 20, beam hardening 41, minimum for CS to Image Conversion=0,000, maximum for CS to Image Conversion=0,03.

Sample № 8

smoothing 2, ring reduction 20, beam hardening 41, minimum for CS to Image Conversion=0,000, maximum for CS to Image Conversion=0,03.

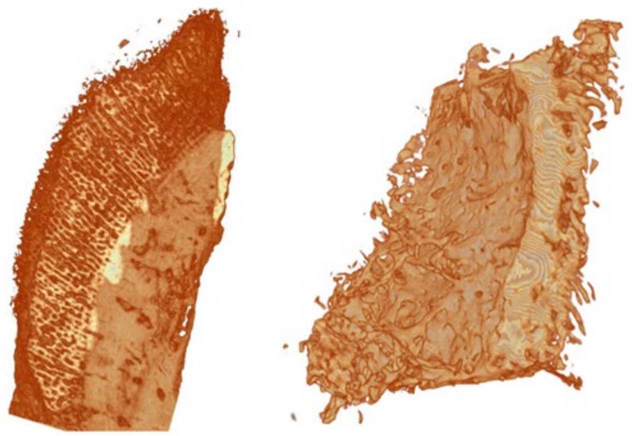

Sample № 1. The bone tissue of a sheep's jaw in normal state.

Sample № 2. The bone tissue of the sheep's jaw in osteoporosis simulation.

Fig.1. Comparison of samples № 1 and № 2.

Table 1

Results of microtomography analysis of sheep jaw bones in osteoporosis simulation

Name of samples	BMD, g/cm³ (bone tissue in trabeculae only)	Tb.Pf (1/mm) *	SMI **
Sample № 1	0,815	-2,35	-0,46
Sample № 2	0,661	9,23	1,75
The difference	**-18,9%**	**на 11,58**	**на 2,21**

*Note: *Trabecular pattern factor, **Structure model index.*

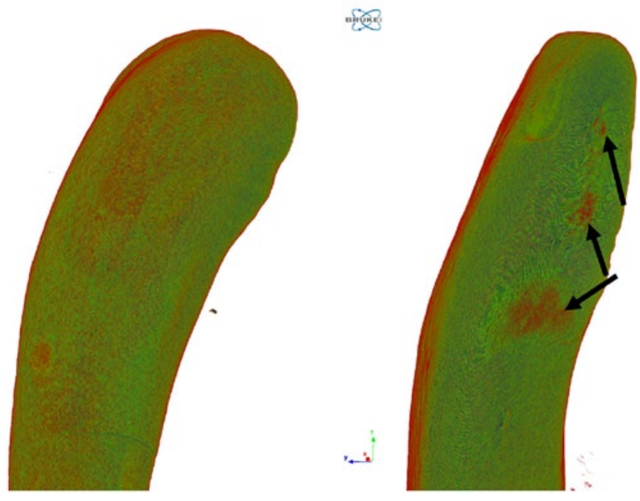

Sample № 3. Sheep's tooth in the normal state

Sample № 4. A sheep's tooth in an osteoporosis simulation. Arrows mark areas of enamel erosion. X-ray density increases from red to green.

Fig. 2. Comparison of samples № 3 and № 4.

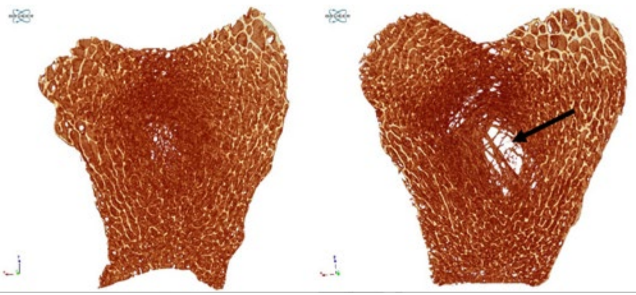

Sample № 5. Trabecular structure in the metaphyseal area of the sheep femur in the normal state.

Sample № 6. Trabecular structure in the metaphyseal region of the sheep femur in the osteoporosis simulation. An arrow marks the area of trabecular elimination, and the formation of few thickened trabeculae is also detected.

Fig. 3. Comparison of samples № 5 and № 6.

Orientation (x, y, z) and isolation of individual regions of reconstructed materials was performed in DataViewer (1.5.6.2, Bruker-microCT, Belgium).

Visualization, data analysis and BMD determination were performed in the CT-analyser software (1.18.4.0, Bruker-microCT, Belgium). According to the manufacturer's official guidelines, the software was first calibrated using phantoms, followed by the BMD determination in the different VOI samples. A 3D-visualisation of the results obtained as a function of radiological density was performed in the CTvox software (3.3.0r1403, Bruker-microCT, Belgium).

Results

Examination of samples by microtomography and 3D-analysis showed a decrease of trabecular tissue mineral density in Sample № 2 by 0.154 g/cm3 (18.9%) (*Fig. 1*), a significant increase of indices, in particular Tb. Pf. and SMI by 11.58 and 2.21 indicating calcium wash-out and thinning of trabeculae, reduction of trabecular connectivity and their transition from plate-like to rod-like architecture (*Tab. 1*). This type of change is characteristic of osteoporosis.

Numerous enamel erosions are visualised in the microCT analysis of the teeth of a sheep in which osteoporosis has been simulated (*Fig. 2*).

The state of osteoporosis was also confirmed by the main method, microtomography of the femur bones of sheep (*Fig. 3*). a 3D-analysis of the metaphysis of the femur of an animal with simulated osteoporosis showed a 15.1% decrease in bone percentage, a 7.8% decrease in bone mineral density as well as an increase in indices, particularly Tb. Sp., Tb. Pf. and SMI by 30.2%, 20.8% and 23.6% respectively and a decrease in Tb.N. index by 18.6% (*Tab. 2*). This indicates

Table 2

Results of microtomography analysis of sheep femurs in osteoporosis simulation

Name of samples	BV/TV,%	BMD, г/cм³	Tb.Th, mm	Tb.N, (1/mm) *	Tb.Sp, mm **	Tb.Pf (1/mm) ***	SMI ****
Sample № 5	23,2	0,284	0,271	0,86	2,25	1,44	0,72
Sample № 6	19,7	0,262	0,283	0,7	2,93	1,74	0,89
The difference	**-15,1%**	**-7,8%**	**+4,4%**	**-18,6%**	**+30,2%**	**+20,8%**	**+23,6%**

*Note: *Trabecular number, **Trabecular separation ***Trabecular pattern factor (Tb. Pf), ****Structure model index (SMI).*

Sample № 7. Trabecular structure of the sheep's iliac bone in normal state.

Sample № 8. Trabecular structure of sheep ileum in osteoporosis simulation.

Fig. 4. Comparison of samples № 7 and № 8.

calcium washout and thinning of the trabeculae, decreased connectivity between the trabeculae, and a change from a lamellar to a rod-like architecture, which is characteristic of osteoporosis.

Moreover, additional 3D-analysis of iliac microtomography (*Fig. 4*), also indicates the development of osteoporosis, which is confirmed by a significant increase of 80.6% and 81.5% in the main indices characterising this pathology, Tb. Pf. and SMI, respectively (*Tab. 3*).

Findings

Examination of samples by microtomography and 3D-analysis showed a decrease of mineral density of trabecular tissue in sample № 2 by 0,154 g/cm3 (18,9%), significant increase of indices, in particular Tb. Pf. and SMI by 11,58 and 2,21 indicating calcium washout and thinning of trabeculae, reduction of the connection level between trabeculae and their change from plate-like to rod-like architecture which is typical for osteoporosis.

Numerous enamel erosions are visualized in the microCT analysis of the teeth of a sheep in which osteoporosis has been simulated.

The condition of osteoporosis was confirmed by the main method, microCT of the femoral bones of sheep. a 3D-analysis of the metaphysis of the femur of the animal with simulated osteoporosis showed a 15.1% decrease in bone percentage, a 7.8% decrease in bone mineral density and an increase in the indices, particularly Tb. Sp, Tb. Pf. and SMI by 30.2%, 20.8% and 23.6%, respectively, and a decrease in Tb. N. index by 18.6%, indicating calcium washout and thinning of the trabeculae, a reduction in the level of communication between the trabeculae and their transition from a lamellar to a rod-like architecture, which is characteristic of osteoporosis.

Moreover, additional 3D-analysis of iliac microtomography also indicates a pattern of osteoporosis, which is confirmed by a significant increase of 80.6% and 81.5% in the main indices characterizing the development of this pathology, Tb. Pf. and SMI, respectively.

Conclusions

The obtained results objectively indicate the development of osteoporosis in experimental animals, but also indicate signs of adaptation-compensatory reactions of the body. These reactions are characterized by the appearance of large trabeculae in the metaphyseal area of the femur, an unexpressed decrease in bone mineral density and bone tissue area, especially in the iliac bone. Such morphological analysis would not have been possible without the use of computed tomography techniques. The conventional methods of histological examination with slices, macro- and microspecimens are not able to quantify the magnitude of osteoporosis and assess the degree of bone deformation. When examining the hard tissues in experimental animals, it is reasonable to use methods of examination without damaging the integrity of the examined samples, because it will be impossible to visualise and reconstruct the qualitative and quantitative indicators of conducted work. It is the objectivity and clarity of this technique that enables us to recommend its use for the evaluation of bone tissue in various experimental studies, so necessary for clinicians of various specialisations.

References

1. Grande, N.M.; Plotino, G.; Gambarini, G.; Testarelli, L.; D'Ambrosio, F.; Pecci, R.; Bedini, R. Present and future in the use of microCT scanner 3D-analysis for the study of dental and root canal morphology. Ann. Ist. Super. Sanità 2012, 48, 26–34.
2. Korzhevsky D. E., Gilyarov A. V. Fundamentals of histological technique.– SPb.: SpetsLit, 2010.– 95 p.
3. Charwat-Pessler, J.; Musso, M.; Petutschnigg, A.; Entacher, K.; Plank, B.; Wernersson, E.; Tangl, S.; Schuller-Gotzburg, P. a bone sample containing a bone graft substitute analyzed by correlating density information obtained by X-ray micro tomography with compositional information obtained by raman microscopy. Materials 2015, 8, 3831–3853.
4. Daly, S.M. Biophotonics for Blood Analysis; Elsevier: Amsterdam, The Netherlands, 2015; ISBN 9780857096746.
5. Campioni, I.; Cacciotti, I.; Gupta, N. Additive manufacturing of reconstruction devices for maxillofacial surgery: Design and accuracy assessment of a mandibular plate prototype. Ann. Ist. Super. Sanità 2020, 56, 10–18.
6. Mangione, F.; Meleo, D.; Talocco, M.; Pecci, R.; Pacifici, L.; Bedini, R. Comparative evaluation of the accuracy of linear measurements between cone beam computed tomography and 3D-microtomography. Ann. Ist. Super. Sanità 2013, 49, 261–265.
7. Sinibaldi, R.; Pecci, R.; Somma, F.; Penna, S.D.; Bedini, R. a new software for dimensional measurements in 3D-endodontic root canal instrumentation. Ann. Ist. Super. Sanità 2012, 48, 42–48.
8. Vögtlin, C.; Schulz, G.; Jäger, K.; Müller, B. Comparing the accuracy of master models based on digital intraoral scanners with conventional plaster casts. Phys. Med. 2016, 1, 20–26.

Table 3

Results of microtomography analysis of sheep iliac bones in osteoporosis simulation

Name of sampes	BV/TV,%	BMD, г/см^3	Tb.Th, mm	Tb.N, (1/mm) *	Tb.Sp, mm **	Tb.Pf (1/mm) ***	SMI****
Sample № 7	26,7	0,331	0,188	1,42	0,71	0,72	0,27
Sample № 8	26,4	0,318	0,192	1,38	0,65	1,3	0,49
The difference	**-1,1%**	**+3,9%**	**+2,1%**	**-2,8%**	**-8,5%**	**+80,6%**	**+81,5%**

*Note: *Trabecular number, **Trabecular separation, ***Trabecular pattern factor (Tb. Pf), ****Structure model index (SMI).*

9. Cengiz, I.F.; Oliveira, J.M.; Reis, R.L. Micro-computed tomography characterization of tissue engineering scaffolds: Effects of pixel size and rotation step. J. Mater. Sci. Mater. Med. 2017, 28.
10. Boerckel, J.D.; Mason, D.E.; McDermott, A.M.; Alsberg, E. Microcomputed tomography: Approaches and applications in bioengineering. Stem Cell Res. Ther. 2014, 5, 1–12
11. Liao, C.-W.; Fuh, L.-J.; Shen, Y.-W.; Huang, H.-L.; Kuo, C.-W.; Tsai, M.-T.; Hsu, J.-T. Self-assembled micro-computed tomography for dental education. PLoS ONE 2018, 13, e0209698.
12. Deyhle, H.; Schmidli, F.; Krastl, G.; Müller, B. Evaluating tooth restorations: Micro-computed tomography in practical training for students in dentistry. Int. Soc. Optical Eng. 2010, 7804, 780417.
13. Sandholzer, M.A.; Walmsley, A.D.; Lumley, P.J.; Landini, G. Radiologic evaluation of heat-induced shrinkage and shape preservation of human teeth using microCT. J. Forensic Radiol. Imaging 2013, 1, 107–111.
14. Rutty, G.N.; Brough, A.; Biggs, M.J.P.; Robinson, C.; Lawes, S.D.A.; Hainsworth, S. V. The role of micro-computed tomography in forensic investigations. Forensic Sci. Int. 2013, 225, 60–66.
15. Leeson, D. The digital factory in both the modern dental lab and clinic. Dent. Mater. 2019, 1, 43–52.
16. Bouxsein M. L., Boyd S. K., Christiansen B. A., Guldberg R. E., Jepsen K. J., Muller R. Guidelines for assessment of bone microstructure in rodents using micro–computed tomography // Journal of Bone and Mineral Research. 2010. Vol. 25, N 7. P. 1468–1486. DOI:10.1002/jbmr.141.

Received 15.07.2022
Revised 18.07.2022
Accepted 23.07.2022

INFORMATION ABOUT AUTHORS

Dolgalev Alexander Alexandrovich, *PhD, MD, Head of the Center for Innovation and Technology Transfer, Professor of the Department of General Practice Dentistry and Pediatric Dentistry of Stavropol State Medical University of the Ministry of Health of the Russian Federation, Professor of the Department of Clinical Dentistry with a course of OS and MFS of Pyatigorsk Medical and Pharmaceutical Institute-branch of the Volgograd State Medical University, Stavropol, Russian Federation. ORCID: https://orcid.org/0000-0002-6352-6750. Tel. +79624404861, e-mail: dolgalev@dolgalev.pro*

Rzhepakovsky Igor Vladimirovich, *Candidate of Biological Sciences, Associate Professor at the Department of Applied Biotechnology, leading researcher of the interdepartmental research and education laboratory of experimental immunomorphology, immunopathology and immunobiotechnology, North-Caucasus Federal University, Stavropol, Russian Federation. Tel. +79054164981, e-mail: irzhepakovskii@ncfu.ru*

Danaev Aslan Baradinovich, *Head of the Saverclinica Centre for Training in the Basics of Lean Manufacturing in Health Care at the institute of additional professional education, Stavropol State Medical University of the Ministry of Health of the Russian Federation, Stavropol, Russian Federation. ORCID: https://orcid.org/0000-0003-4754-3101. Tel. +79289111148, e-mail: aslandanaev111@mail.ru*

Avanisyan Vazgen Mikhailovich, *the 5-th grade student of the Faculty of Dentistry of the Stavropol State Medical University of the Ministry of Health of the Russian Federation, Stavropol, Russian Federation. ORCID: https://orcid.org/0000-0002-0316-5957. Tel. +79286338995, e-mail: avanvaz@yandex.ru*

Shulga Galina Sergeevna, *the 4-th grade student of the Faculty of Dentistry of the Stavropol State Medical University of the Ministry of Health of the Russian Federation, Stavropol, Russian Federation. ORCID: https://orcid.org/0000-0003-2328-6948. Tel. +79288266451 e-mail: g.dolgopolowa2015@yandex.ru*

Korobkeev Artemy Aleksandrovich, *the 3-th grade student of the Faculty of Dentistry of the Stavropol State Medical University of the Ministry of Health of the Russian Federation, Stavropol, Russian Federation. ORCID: https://orcid.org/0000-0001-6188-2578. Tel. +79624429874, e-mail: korobkeevartemy@gmail.com*

DOI:10.33667/2782-4101-2022-2-21-26

TISSUE–ENGINEERED BONE IMPLANTS FOR THE REPLACEMENT OF JAWBONE DEFECTS. LITERATURE REVIEW

Konstantin Kobets, Artak Kazaryan, Saddam Bopkhoev

Peoples' Friendship University of Russia (RUDN University), 6 Miklukho-Maklaya St., Moscow, 117198, Russian Federation

SUMMARY
The purpose of the study: *to trace the development of methods of bone implants for the replacement of jawbone defects: from ceramic and polymeric scaffolds to complex tissue-engineered structures with stem cells, growth factors and vascular anastomoses based on literature data.*
Materials and methods: *searching, systematization and analysis of scientific data on various types of 3D-printed bone implants and their effectiveness in replacing bone defects.*
Conclusions: *Modern technologies of 3D-printing, cell and tissue engineering, microvascular surgical techniques closely approach scientists and clinicians to creation of an artificial bone implant which in the body must become a living structure capable of integrating with the patient's bone. Only complex approach which includes reconstruction of the implant of individual shape and sufficient mechanical strength, giving of osteoinductive and osteogenic properties, providing of internal axial and external angiogenesis is the basis for such tissue-engineered construction.*

KEYWORDS: *artificial tissue implants, bone vascularisation, bone implants, bone engineering, bone the defects reconstruction, arteriovenous loop.*

CONFLICT of INTEREST. *The authors declare no conflict of interest.*

Introduction

Tissue damage caused by trauma, cancer and infectious processes can lead to extensive defects and deformities requiring reconstructive surgery. More than 500,000 people with head and neck cancers are identified each year (Cohen et al., 2018). Modern surgical treatment of malignant lesions implies one-stage removal of resection defects. For this purpose, vascularized bone or combined bone-soft tissue autografts are the «gold standard» [Huang et al. [Huang et al., 2016]. For example, for mandibular reconstruction, the peroneal autograft on microvascular anastomosis is most often used. Its advantages are a long vascular stem, vessel diameter, suitable length and thickness of the bone, the possibility of performing reconstruction over a long distance, the possibility of including a muscle or skin component with a flap, stable bone structure that allows intraosseous implantation and further orthopedic prosthesis, minimal resorption [Tereshchuk et al., 2018].

However, all autotransplant surgeries have disadvantages and limitations. First, it is an additional surgical procedure of graft taking, defect or instability of the donor site, deformation and pain in the donor site, risk of infection (Lakhiani et al., 2016; Simon et al., 2003; Hartman et al., 2002). The main factor determining the nutrition and «survival» of the graft at the microvascular anastomosis is the patency of the anastomosis itself. This can be influenced by surgical technique, anaesthetic and medication support, and postoperative regimen.

Despite the impressive success of microsurgical procedures in tissue and organ transplantation, the development of artificial tissue-engineered constructs to replace bone and other tissue defects is a promising area. Advances in cell engineering (the ability to cultivate deterministic cells), genetics and molecular biology (synthesis of cytokines and growth factors), 3D-printing of matrices and scaffolds of the right shape with biocompatible materials facilitate this.

This review focuses on current advances in tissue engineering in the development of vascularised tissue implants (VTIs), especially bone implants. The requirements for VTIs are described and systematised, the technologies for VTI creation are reviewed and the results of their use *in in vivo* experiments are given.

Materials and methods

The scientific literature for this review was collected from the following on-line databases and libraries: https://elibrary.ru/, https://scholar. google. ru/, https://pubmed. ncbi. nlm. nih. gov, https://www. sciencedirect. com/. Search was performed using the following keywords: artificial tissue implants, bone vascularization, bone implants, bone engineering, bone defect reconstruction, arteriovenous loop; no date restrictions.

Discussion

3D-prototyping of bone implant

Currently, it is possible to produce a biocompatible bone implant (scaffold) of any geometric shape, including an individual one for each particular patient using 3D-printing [Tereshchuk S. V. et al., 2019, Kim et al., 2021].

Due to the nature of the material used for 3D-printing and the architectonics of 3D-printing, bone implants usually have osteoconductive properties, i. e. they are a matrix for bone tissue formation on their basis. Adding growth factors, cytokines and cells to their composition can additionally give osteoinductive and osteogenic properties [Muraev A. A. et al., 2013].

Thus the usage of biphasic calcium phosphate as a scaffold is much more effective than using pure hydroxyapatite and beta-tricalcium phosphate (HA and b-TCP) [Kohri M et al., 1993; Nery et al., 1992]. The pores and their number and size in the scaffold play an important role in the process of surrounding tissue ingrowth into the material and the osseointegration of the material. If the pore size is below 100 μm, fibrovascular encapsulation of the implant may occur; 100–500 μm is considered optimal [Kühne et al. 1994].

In addition to its effect on the regeneration of the bone tissue itself, pore size affects vascular growth, which is more pronounced in large pores (Druecke D et al., 2004).

It is important to understand that in order for a complete bone implant to form, a vascular structure must be formed in its structure to nourish it.

External and internal vascularisation

Vascularisation is a key link in the growth of new and regeneration of damaged tissue. When creating osteoplastic materials for the replacement of small bone defects, vascular endothelial growth factor (VEGF) may be included in the material composition. Thanks to VEGF a well-developed microcirculatory channel is formed in the regeneration zone [Muraev A. A. et al., 2012; 2012].

This approach refers to external neovascularisation, i. e., the microvascular bed is «connected» to existing adjacent

Results of the study

	https://elibrary.ru/	https://scholar. google. ru/	https://pubmed.ncbi.nlm.nih.gov	https://www.sciencedire ct. com/.
Artificial tissue implants	1	45	8198	15
Bone vascularisation	35	1850	97	1347
Bone implants	1248	32200	1034	14609
Bone engineering	256	11300	373	988
Bone defect reconstruction	42	2030	179	294
Arteriovenous loop	49	2520	210	520

arterioles. This type of neovascularization is ineffective when the size of the bone defect is large and in places that have been exposed to radiation [Lokmic Z et al, 2006; Tanaka et al, 2000]. This is the reason why the formation, development and survival of new cells in the centre of large constructions is limited at the beginning of vascularisation. If when a scaffold is implanted into an area where there is good vascularisation there will be development of a vascular network, then further transplantation into the recipient area will result in cessation of blood supply, as there is no subsequent connection to the vascular network in the defect site.

These problems have led to the development of new methods of neoangiogenesis for artificial tissue-engineered constructs, namely internal vascularisation. Internal vascularization is a method in which an artery or vein serves as a source of new vessels for tissue creation, which further allows the implant to be transferred to the recipient area by means of microvascular anastomoses [Tanaka Y et al., 2003; Erol et al., 1980; Khouri et al., 1991].

As mentioned above, 3D-printing allows the creation of artificial implants of defined macro- and micro-architecture. Therefore, the next step, in order to provide internal vascularisation, was to prefabricate channels for the vascular bed within the bone implant. With the prefabrication techniques it is possible to obtain the desired vascularised flap with an axial type from a flap with incidental vascularisation. With the arteriovenous loop it has become possible to implant grafts in highly vascularised areas and after a certain period to graft with connection to the local vascular network with microvascular anastomoses for tissue and cell feeding.

3D-printing of the channels for the new vessels should be guided by the structure of the vascular bed of the jawbone tissue and the surrounding vessels. The diameter of the lingual artery is 2.3±0.1 mm, the facial artery is 2.2±0.2 mm, the diameter of the maxillary artery is 3.3±0.3 cm [Lukyanov V. G. 1971] According to Jiang G. H. et al. the diameter of the left facial artery is 1.4–4.7 mm (mean 2.83±0.77 mm), the right one is 1.6–4.3 mm (mean 2.81±0.79 mm) [Jiang et al., 2008].

Volikov V. V. described the structure of the microvascular system of the maxilla alveolar process in norm and in case of tooth loss. Thus, in the presence of all teeth, the vascular system is represented by tubular structures with a rounded cross-section, located mostly perpendicular to the bone surface, with numerous anastomoses. The vascularisation of the bone tissue is satisfactory. The arterial vessels have a thin wall.

The diameter of the veins exceeds the diameter of the arteries by 2–4 times. Morphometric analysis of the periodontal vessels revealed that in intact dentition the number of vessels in 1 sq.mm. in the projection of the 11th tooth was 18,25 ± 3,58, in the projection of the 21st tooth – 19,05 ± 3,26, in the projection of the 16th tooth – 19,10 ± 4,01, in the projection of the 26th tooth – 19,30 ± 3,27 (at $p<0,05$). In the projection of all studied teeth the number of vessels in 1 sq.mm. was more in women in comparison with men. In comparison with the group of patients with intact dentition in partial and total adentia the number of vessels in 1 sq.mm. decreased by 20 % and 60 % respectively, vessel diameter was 40 % and 70 %, the thickness of the vascular wall increased by 2 and 4 times respectively. [Volikov V. V. et al., 2015].

Revascularised bone implants

The next step in the evolution of artificial bone implants (ABI) was to combine the tissue-engineered structure with living vessels by introducing a main feeding vessel into them. As such a vessel an arteriovenous loop or a vascular stalk is used, which is placed directly in the bone implant (BI) or under it. It was shown that the feeding vessel allows good vascularization of the BI, due to the formation of a microcirculatory channel around it [Khouri et al. 1991; Tan et al., 2004; Hirase et al., 1987; Morrison et al., 1990]. Such work is actively carried out *in vivo* on animal models. For this purpose the highly vascularized regions are chosen, where the prefabricated BI is placed and after some time it is transferred into the bone defect with the connection to the local vascular network with the help of the microvascular anastomoses. The vascular axis becomes a supporting vessel after transplantation and microsurgical anastomoses with the local vessels to allow the new vessels to live and integrate.

As an axial vessel, the arteriovenous loop has proven most effective (Tanaka et al., 2003; Cassell et al., 2002; Kneser et al., 2006).

Because of mechanical stimulation, the level of VEGF (vascular endothelial growth factor) increases when a vascular graft is introduced into the arterial circulation (Nath et al., 2003; Dvorak et al., 1995). The local inflammatory reaction that occurs during surgical intervention on a vessel causes an angiogenic reaction. VEGF levels in platelets increase under the influence of proinflammatory chemokines [Nath et al., 2003]. In microvascular anastomoses there is an increase in endothelial cells in microvascular anastomoses due to the combination of blood shear stress and turbulent current changes [Davies et al., 1986].

Once the main vessel in the BI is integrated and the vascularisation process is complete, the BI is transferred to the recipient area to repair the bone defect and connected to the recipient vessel. By 8 weeks, there is significant vascularisation of the matrix with an arteriovenous loop (Kneser et al., 2006).

Arteriovenous loop

An arteriovenous loop (AVP) is a pathological direct connection between an artery and a vein (congenital or acquired), creating blood flow bypassing the capillary network. Pathological to normal tissues, in the experiment AVP promoted flow-induced axial vascularisation. Thus, placed in the central part of the bone implant, AVP is a source of «axial vascularization», which in combination with peripheral angiogenesis («external vascularization») provides adequate blood supply and thus opens significant prospects in solving the problem of increasing the survival of cells comprising the BI [Leibig et al., 2016].

In 1980, Erol and Spira developed the arteriovenous loop method (AVP) in experimental animals [Erol et al., 1980;]. The authors used rats weighing 250–350 grams. An artery and vein were exposed on one side of the femoral vessels, and a venous graft was obtained on the other side. Next, the vessels were prepared by ligating the proximal part of the vein and the distal end of the artery. The venous graft was washed with heparin and then two end-to-end anastomoses were applied: the proximal end of the artery and the distal end of the vein. The criterion of the vessel patency was the pulsation of the venous loop. The loop was inserted into the implantation chamber and then closed from above with the second part of the implant. The chamber was closed and tied with 6/0 non-absorbable sutures. The skin was sutured 4/0–5/0. Postoperatively, heparin was injected intravenously. IVG (interpositional vein grafts) is necessary to avoid tension in the loop between the artery and vein, and is a good inducer for early angiogenesis (Polykandriotis et al., 2007; Schmidt et al., 2013). The loop is completely isolated, allowing vascularisation at the expense of the AV loop. This results in hypoxia in the chamber, which is a stimulus for neoangiogenesis. Hypoxia and cell proliferation reach their peak on day 7 [Lokmic Z et al, 2006].

Experiments using the arteriovenous loop method are also possible in other animals such as rabbits, dogs, sheep [Wu X et al., 2015; Eweida et al., 2017; Dong et al., 2012]. Experiments on larger animals have provided the rationale for the clinical use of the method.

AVP has been used in various experimental models. To create the BIs, the AVP method was combined with different scaffolds, including growth factors and cells: mesenchymal stem cells (MSCs) [Arkudas et al., 2017; Kim HY et al., 2018; Boos et al., 2012; Buehrer et al., 2014] or osteoblasts [Arkudas et al., 2007]. For cell differentiation, a number of authors have added specific growth factors to CIs. The combination of MSCs (mesenchymal stem cells) and BMP-2 (Bone morphogenetic protein-2) leads to accelerated bone development in the AB loop [Buehrer et al., 2014].

There are studies that focus on the possibility of growth of muscle tissue, heart tissue, soft tissue, lymphatic vessels and internal organs [Tee et al., 2012; Messina et al., 2005; Witt et al., 2017; Fiegel et al., 2008; Brown et al., 2006; Robering et al., 2018].

Work on lymphatic vessels is at a very early stage and clinically very much in demand, with Jan Robering working on lymphatic tissue development using an AV loop [Robering et al., 2018].

Bone implants can be different in sizes, depending on the zone of the defect, the size of the AVP is chosen according to its size (Cassell et al., 2001; Hofer et al., 2003). It has been shown that creation of additional external perforations in the BI results in faster vascular growth from the surrounding implant tissues [Dolderer et al., 2010]. Thus, in perforated implants there is an increase in angiogenesis in the arteriovenous loop due to the connection to the additional external vascular network, which significantly reduces the time of pre-vascularization and tissue formation [Arkudas et al., 2012].

Preclinical *in vivo* studies on large animals using a long AVP and large BIs of clinically relevant size can be considered. Justus Beier et al. in a study on sheep formed an AVP using a saphenous artery and femoral vein in a large model, with an implant size of 2.8 cm long, 1.8 cm wide and 1.8 cm high and with a volume of 16 cm [Beier et al., 2009]. Wu X in a study on dogs formed an AVP from the saphenous artery and femoral vein, which allowed the IVG not to be used [Wu X et al., 2015]. The success of this technique has also been shown in rabbits using the saphenous artery and femoral vein [Eweida et al., 2017].

Studies have shown that the less flexion of the AVP, the less likely to develop thrombosis, also the non-use of IVG (interpositional vein grafts) simultaneously with saphenous artery and femoral vein anastomosis is possible, as the anastomosis length between the artery and vein is sufficient and there is no tension [Dong et al, 2012; Weigand et al., 2015; Eweida et al., 2013]. However, several studies show that IVG (interpositional vein grafts) is an important factor in angiogenesis [Polykandriotis et al., 2007; Schmidt et al., 2013].

There may be a reduced risk of thrombosis with the AV-beam, less surgical experience is possible with this technique, but studies show that the loop is more effective for angiogenesis within the scaffold. The vascular bundle has a lower degree of vascularisation but better balance between the bone formation and the scaffold [Rudolph et al., 2020].

Conclusion

Modern 3D-printing, cell and tissue engineering and microvascular surgical techniques have brought scientists and clinicians closer to the creation of an artificial bone implant, which in the body must become a living structure capable of integrating with the patient's bone. Only a comprehensive approach that includes recreating an implant with an individual shape and sufficient mechanical strength, imparting osteoinductive and osteogenic properties, ensuring internal axial and external angiogenesis, is basic for such a tissue-engineered structure.

References

1. *Cohen N, Fedewa S, Chen AY. Epidemiology and Demographics of the Head and Neck Cancer Population. Oral Maxillofac Surg Clin North Am. 2018 Nov;30(4):381–395. Doi: 10.1016/j.coms.2018.06.001. Epub 2018 Aug 3. PMID: 30078696.*
2. *Huang RL, Kobayashi E, Liu K, Li Q. Bone Graft Prefabrication Following the In Vivo Bioreactor Principle. Ebiomedicine. 2016 Oct;12:43–54. Doi:10.1016/j.ebiom.2016.09.016. Epub 2016 Sep 20. PMID: 27693103; PMCID: PMC5078640.*
3. *Tereshchuk S, Sukharev V. Refined Approach to Preservation of the Inferior Alveolar Nerve during Resection and Primary Reconstruction of the Mandible. Craniomaxillofac Trauma Reconstr. 2019 Mar;12(1):34–38. Doi: 10.1055/s-00381639348. Epub 2018 Mar 28. PMID: 30815213; PMCID: PMC6391257.*
4. *Lakhiani C, defazio MV, Han K, Falola R, Evans K. Donor-Site Morbidity Following Free Tissue Harvest from the Thigh: a Systematic Review and Pooled Analysis of Complications. J Reconstr Microsurg. 2016 Jun;32(5):342–57. Doi: 10.1055/s-0036–1583301. Epub 2016 May 4. PMID: 27144952.*
5. *Rogers SN, Lakshmiah SR, Narayan B, Lowe D, Brownson P, Brown JS, Vaughan ED. A comparison of the long-term morbidity following deep circumflex iliac and fibula free flaps for reconstruction following head and neck cancer. Plast Reconstr Surg. 2003 Nov;112(6):1517–25; discussion 1526–7. Doi: 10.1097/01.PRS.0000082817.26407.86. PMID: 14578779.*

6. Hartman EH, Spauwen PH, Jansen JA. Donor-site complications in vascularized bone flap surgery. J Invest Surg. 2002 Jul-Aug;15(4):185–97. Doi: 10.1080/08941930290085967. PMID: 12217183.
7. Tereshchuk S. V., Ivanov S. Y., Sukharev V. A., Role of adaptive technologies in modern reconstructive chirogy, Military Medical Journal. 2019. T. 340. № 10. C. 28–32.
8. Kim EV, Petronyuk YS, Guseynov NA, Tereshchuk SV, Popov AA, Volkov AV, Gorshenev VN, Olkhov AA, Levin VM, Dymnikov AB, Rodionov VE, Tumanyan GA, Ivashkevich SG, Bonartsev AP, Borozdkin LL. Biocompatibility and Bioresorption of 3D-Printed Polylactide and Polyglycolide Tissue Membranes. Bull Exp Biol Med. 2021 Jan;170(3):356–359. Doi: 10.1007/s10517–021–05066-x. Epub 2021 Jan 16. PMID: 33452990.
9. Muraev A. A. et al., Ivanov S. Yu., Kibardin A., Dymnikov A. B., Larin S. S. Possibilities of creating bioceramic bone substituting materials by 3D-prototyping», Proceedings of III International Scientific and Practical Conference «New Technologies of Bioceramics Creation and Application in Regenerative Medicine»; Tomsk Polytechnic University.– Tomsk: Tomsk Polytechnic University Press, 2013, pp. 120–124
10. Kohri M, Miki K, Waite DE, Nakajima H, Okabe T. In vitro stability of biphasic calcium phosphate ceramics. Biomaterials. 1993;14(4):299–304. Doi: 10.1016/0142–9612(93)90122-i. PMID: 8386558.
11. Nery EB, legeros RZ, Lynch KL, Lee K. Tissue response to biphasic calcium phosphate ceramic with different ratios of HA/beta TCP in periodontal osseous defects. J Periodontol. 1992 Sep;63(9):729–35. Doi: 10.1902/jop.1992.63.9.729. PMID: 1335498.
12. Kühne JH, Bartl R, Frisch B, Hammer C, Jansson V, Zimmer M. Bone formation in coralline hydroxyapatite. Effects of pore size studied in rabbits. Acta Orthop Scand. 1994 Jun;65(3):246–52. Doi: 10.3109/17453679408995448. PMID: 8042473.
13. Druecke D, Langer S, Lamme E, Pieper J, Ugarkovic M, Steinau HU, Homann HH. Neovascularization of poly(ether ester) block-copolymer scaffolds in vivo: long-term studies using intravital fluorescent microscopy. J Biomed Mater Res A. 2004 Jan 1;68(1):10–8. Doi: 10.1002/jbm.a.20016. PMID: 14661244.
14. Muraev A. A., Ivanov S. Y., Artifexova A. A., Ryabova V. M., Volodina E. V., Polyakova I. N. Study of biological properties of new osteoplastic material based on non-mineralized collagen containing vascular endothelial growth factor in bone defects replacement // Modern technologies in medicine, ¹ 1, 2012, pp. 21–26.;
15. Muraev A. A., Ivanov S. Y., Ryabova V. M., Artifexova F. F., Volodina E. V., Polyakova I. N. Toxicity and biological activity of a new osteosubstituting material based on non-mineralized collagen containing vascular endothelial growth factor. // Modern technologies in medicine, № 3, 2012, p. 19–26
16. Lokmic Z, Stillaert F, Morrison WA, Thompson EW, Mitchell GM. An arteriovenous loop in a protected space generates a permanent, highly vascular, tissueengineered construct. FASEB J. 2007 Feb;21(2):511–22. Doi: 10.1096/fj.06–6614com. Epub 2006 Dec 16. PMID: 17172640.
17. Tanaka Y, Tsutsumi A, Crowe DM, Tajima S, Morrison WA. Generation of an autologous tissue (matrix) flap by combining an arteriovenous shunt loop with artificial skin in rats: preliminary report. Br J Plast Surg. 2000 Jan;53(1):51–7. Doi: 10.1054/bjps.1999.3186. PMID: 10657450.
18. Tanaka Y, Sung KC, Tsutsumi A, Ohba S, Ueda K, Morrison WA. Tissue engineering skin flaps: which vascular carrier, arteriovenous shunt loop or arteriovenous bundle, has more potential for angiogenesis and tissue generation. Plast. Reconstr. Surg. 2003 Nov;112(6):1636–44. Doi: 10.1097/01.PRS.0000086140.49022.AB. PMID: 14578795.
19. Erol OO, Sira M. New capillary bed formation with a surgically constructed arteriovenous fistula. Plast Reconstr Surg. 1980 Jul;66(1):109–15. Doi: 10.1097/00006534–198007000–00021. PMID: 6156468.
20. Khouri RK, Upton J, Shaw WW. Prefabrication of composite free flaps through staged microvascular transfer: an experimental and clinical study. Plast Reconstr Surg. 1991 Jan;87(1):108–15. Doi: 10.1097/00006534–199101000–00017. PMID: 1984254.
21. Lukyanov V. G. Intraorgan relationships of vessels and nerves of periosteum of upper and lower jaws / V. G. Lukyanov // Dentistry.– 1971.– № 2.– C. 82–85.
22. Jiang GH, Yan JH, Lin CL, Huang Y, Wen H, Li WM. [Anatomic study of the facial artery using multislice spiral CT angiography]. Nan Fang Yi Ke Da Xue Xue Bao. 2008 Mar;28(3):457–9. Chinese. PMID: 18359713.
23. Volikov V. V., Andreeva I. V. Morphological peculiarities of arteries and vasculature of maxillary mandibular paradontium in intact dentition, partial and complete adentia // Materials of annual scientific conference of Academician I. P. Pavlov Ryazan State Medical University, dedicated to the 65th anniversary of the university in the Ryazan region. Ryazan: 2015 P. 272–274
24. Tan BK, Chen HC, He TM, Song IC. Flap prefabrication – the bridge between conventional flaps and tissue-engineered flaps. Ann Acad Med Singap. 2004 Sep;33(5):662–6. PMID: 15536673.
25. Hirase Y, Valauri FA, Buncke HJ, Newlin LY. Customized prefabricated neovascularized free flaps. Microsurgery. 1987;8(4):218–24. Doi: 10.1002/micr.1920080410. PMID: 3323773.
26. Morrison WA, Dvir E, Doi K, Hurley JV, Hickey MJ, O'Brien BM. Prefabrication of thin transferable axial-pattern skin flaps: an experimental study in rabbits. Br J Plast Surg. 1990 Nov;43(6):645–54. Doi: 10.1016/0007–1226(90)90184–2. PMID: 1701673.
27. Cassell OC, Hofer SO, Morrison WA, Knight KR. Vascularisation of tissue-engineered grafts: the regulation of angiogenesis in reconstructive surgery and in disease states. Br J Plast Surg. 2002 Dec;55(8):603–10. Doi: 10.1054/bjps.2002.3950. PMID: 12550111.
28. Kneser U, Polykandriotis E, Ohnolz J, Heidner K, Grabinger L, Euler S, Amann KU, Hess A, Brune K, Greil P, Stürzl M, Horch RE. Engineering of vascularized transplantable bone tissues: induction of axial vascularization in an osteoconductive matrix using an arteriovenous loop. Tissue Eng. 2006 Jul;12(7):172131. Doi: 10.1089/ten.2006.12.1721. PMID: 16889503.
29. Nath KA, Kanakiriya SK, Grande JP, Croatt AJ, Katusic ZS. Increased venous proinflammatory gene expression and intimal hyperplasia in an aorto-caval fistula model in the rat. Am J Pathol. 2003 Jun;162(6):2079–90. Doi: 10.1016/S00029440(10)64339–8. PMID: 12759262; PMCID: PMC1868137.
30. Dvorak HF, Detmar M, Claffey KP, Nagy JA, van de Water L, Senger DR. Vascular permeability factor/vascular endothelial growth factor: an important mediator of angiogenesis in malignancy and inflammation. Int Arch Allergy Immunol. 1995 May-Jun;107(1–3):233–5. Doi: 10.1159/000236988. PMID: 7542074.
31. Davies PF, Remuzzi A, Gordon EJ, Dewey CF Jr, Gimbrone MA Jr. Turbulent fluid shear stress induces vascular endothelial cell turnover in vitro. Proc Natl Acad Sci U S A. 1986 Apr;83(7):2114–7. Doi: 10.1073/pnas.83.7.2114. PMID: 3457378; PMCID: PMC323241.
32. Leibig N, Wietbrock JO, Bigdeli AK, Horch RE, Kremer T, Kneser U, Schmidt VJ. Flow-Induced Axial Vascularization: The Arteriovenous Loop in Angiogenesis and Tissue Engineering. Plast Reconstr Surg. 2016 Oct;138(4):825–835. Doi: 10.1097/PRS.0000000000002554. PMID: 27673517.
33. Polykandriotis E, Tjiawi J, Euler S, Arkudas A, Hess A, Brune K, Greil P, Lametschwandtner A, Horch RE, Kneser U. The venous graft as an effector of early angiogenesis in a fibrin matrix. Microvasc Res. 2008 Jan;75(1):25–33. Doi: 10.1016/j.mvr.2007.04.003. Epub 2007 Apr 18. PMID: 17544455.
34. Schmidt VJ, Hilgert JG, Covi JM, Weis C, Wietbrock JO, de Wit C, Horch RE, Kneser U. High flow conditions increase connexin43 expression in a rat arteriovenous and angioinductive loop model. Plos One. 2013 Nov 13;8(11): e78782. Doi: 10.1371/journal.pone.0078782. PMID: 24236049; PMCID: PMC3827249.
35. Wu X, Wang Q, Kang N, Wu J, Gu C, Bi J, Lv T, Xie F, Hu J, Liu X, Cao Y, Xiao R. The effects of different vascular carrier patterns on the angiogenesis and osteogenesis of BMSC-TCP-based tissue-engineered bone in beagle dogs. J Tissue Eng Regen Med. 2017 Feb;11(2):542–552. Doi: 10.1002/term.2076. Epub 2015 Aug 7. PMID: 26251084.
36. Eweida A, Fathi I, Eltawila AM, Elsherif AM, Elkerm Y, Harhaus L, Kneser U, Sakr MF. Pattern of Bone Generation after Irradiation in Vascularized Tissue Engineered Constructs. J Reconstr Microsurg. 2018 Feb;34(2):130–137. Doi: 10.1055/s-0037–1607322. Epub 2017 Oct 30. PMID: 29084413.
37. Dong QS, Shang HT, Wu W, Chen FL, Zhang JR, Guo JP, Mao TQ. Prefabrication of axial vascularized tissue engineering coral bone by an arteriovenous loop: a better model. Mater Sci Eng C Mater Biol Appl. 2012 Aug 1;32(6):1536–41. Doi: 10.1016/j.msec.2012.04.039. Epub 2012 Apr 28. PMID: 24364957.
38. Arkudas A, Lipp A, Buehrer G, Arnold I, Dafinova D, Brandl A, Beier JP,, Körner C, Lyer S, Alexiou C, Kneser U, Horch RE. Pedicled Transplantation of Axially Vascularized Bone Constructs in a Critical Size Femoral Defect. Tissue Eng Part A. 2018 Mar;24(5–6):479–492. Doi: 10.1089/ten.TEA.2017.0110. Elpub 2017 Oct 25. PMID: 28851253.
39. Kim HY, Lee JH, Lee HAR, Park JS, Woo DK, Lee HC, Rho GJ, Byun JH, Oh SH. Sustained Release of BMP-2 from Porous Particles with Leaf-Stacked Structure for Bone Regeneration. ACS Appl Mater Interfaces. 2018 Jun 27;10(25):21091–21102. Doi: 10.1021/acsami.8b02141. Epub 2018 Jun 12. PMID: 29863327.
40. Boos AM, Loew JS, Weigand A, Deschler G, Klumpp D, Arkudas A, Bleiziffer O, Gulle H, Kneser U, Horch RE, Beier JP. Engineering axially vascularized bone in the sheep arteriovenous-loop model. J Tissue Eng Regen Med. 2013 Aug;7(8):654–64. Doi: 10.1002/term.1457. Epub 2012 Mar 22. PMID: 22438065.

41. Buehrer G, Balzer A, Arnold I, Beier JP, Koerner C, Bleiziffer O, Brandl A, Weis C, Horch RE, Kneser U, Arkudas A. Combination of BMP2 and mscs significantly increases bone formation in the rat arteriovenous loop model. Tissue Eng. Part A. 2015 Jan;21(1–2):96–105. Doi: 10.1089/ten.TEA.2014.0028. Epub 2014 Nov 7. PMID: 25135080; PMCID: PMC4293096.

42. Arkudas A, Beier JP, Heidner K, Tjiawi J, Polykandriotis E, Srour S, Sturzl M, Horch RE, Kneser U. Axial prevascularization of porous matrices using an arteriovenous loop promotes survival and differentiation of transplanted autologous osteoblasts. Tissue Eng. 2007 Jul;13(7):1549–60. Doi: 10.1089/ten.2006.0387. PMID: 17518756.

43. Tee R, Morrison WA, Dusting GJ, Liu GS, Choi YS, Hsiao ST, Dilley RJ. Transplantation of engineered cardiac muscle flaps in syngeneic rats. Tissue Eng Part A. 2012 Oct;18(19–20):1992–9. Doi: 10.1089/ten.TEA.2012.0151. Epub 2012 Sep 4. PMID: 22793168; PMCID: PMC3463279.

44. Messina A, Bortolotto SK, Cassell OC, Kelly J, Abberton KM, Morrison WA. Generation of a vascularized organoid using skeletal muscle as the inductive source. FASEB J. 2005 Sep;19(11):1570–2. Doi: 10.1096/fj.04–3241fje. Epub 2005 Jul 12. PMID: 16014398.

45. Witt R, Weigand A, Boos AM, Cai A, Dippold D, Boccaccini AR, Schubert DW, Hardt M, Lange C, Arkudas A, Horch RE, Beier JP. Mesenchymal stem cells and myoblast differentiation under HGF and IGF-1 stimulation for 3D-skeletal muscle tissue engineering. BMC Cell Biol. 2017 Feb 28;18(1):15. Doi: 10.1186/s12860–0170131–2. PMID: 28245809; PMCID: PMC5331627.

46. Fiegel HC, Pryymachuk G, Rath S, Bleiziffer O, Beier JP, Bruns H, Kluth D, Metzger R, Horch RE, Till H, Kneser U. Foetal hepatocyte transplantation in a vascularized AV–Loop transplantation model in the rat. J Cell Mol Med. 2010 Jan;14(1–2):267–74. Doi: 10.1111/j.1582–4934.2008.00369.x. Epub 2008 May 24. PMID: 18505475; PMCID: PMC3837593.

47. Brown DL, Meagher PJ, Knight KR, Keramidaris E, Romeo-Meeuw R, Penington AJ, Morrison WA. Survival and function of transplanted islet cells on an in vivo, vascularized tissue engineering platform in the rat: A pilot study. Cell Transplant. 2006;15(4):319–24. Retraction in: Morrison WA. Cell Transplant. 2008;16(10):1071. PMID: 16898225.

48. Robering JW, Weigand A, Pfuhlmann R, Horch RE, Beier JP, Boos AM. Mesenchymal stem cells promote lymphangiogenic properties of lymphatic endothelial cells. J Cell Mol Med. 2018 Aug;22(8):3740–3750. Doi: 10.1111/jcmm.13590. Epub 2018 May 11. PMID: 29752774; PMCID: PMC6050462.

49. Cassell OC, Morrison WA, Messina A, Penington AJ, Thompson EW, Stevens GW, Perera JM, Kleinman HK, Hurley JV, Romeo R, Knight KR. The influence of extracellular matrix on the generation of vascularized, engineered, transplantable tissue. Ann N Y Acad Sci. 2001 Nov;944:429–42. Doi: 10.1111/j.17496632.2001.tb03853.x. PMID: 11797691.

50. Hofer SO, Knight KM, Cooper-White JJ, O'Connor AJ, Perera JM, romeomeeuw R, Penington AJ, Knight KR, Morrison WA, Messina A. Increasing the volume of vascularized tissue formation in engineered constructs: an experimental study in rats. Plast Reconstr Surg. 2003 Mar;111(3):1186–92; discussion 1193–4. Doi: 10.1097/01.PRS.0000046034.02158.EB. PMID: 12621190.

51. Dolderer JH, Kehrer A, Schiller SM, Schröder UH, Kohler K, Schaller HE, Siegel-Axel D. De-novo Generierung von vaskularisiertem Gewebe mittels unterschiedlicher Gefässstielkonfigurationen in perforierten und geschlossenen Wachstumskammern [De-novo generation of vascularized tissue using different configurations of vascular pedicles in perforated and closed chambers]. Wien Med Wochenschr. 2010 Mar;160(5–6):139–46. German. Doi: 10.1007/s10354–009–0734–0. PMID: 20364417.

52. Arkudas A, Pryymachuk G, Beier JP, Weigel L, Körner C, Singer RF, Bleiziffer O, Polykandriotis E, Horch RE, Kneser U. Combination of extrinsic and intrinsic pathways significantly accelerates axial vascularisation of bioartificial tissues. Plast Reconstr Surg. 2012 Jan;129(1):55e-65e. Doi: 10.1097/PRS.0b013e3182361f97. PMID: 22186585.

53. Beier JP, Horch RE, Arkudas A, Polykandriotis E, Bleiziffer O, Adamek E, Hess A, Kneser U. De novo generation of axially vascularized tissue in a large animal model. Microsurgery. 2009;29(1):42–51. Doi: 10.1002/micr.20564. PMID: 18853419.

54. Weigand A, Beier JP, Hess A, Gerber T, Arkudas A, Horch RE, Boos AM. Acceleration of vascularized bone tissue-engineered constructs in a large animal model combining intrinsic and extrinsic vascularization. Tissue Eng Part A. 2015 May;21(9–10):1680–94. Doi: 10.1089/ten.TEA.2014.0568. Epub 2015 Apr 15. PMID: 25760576.

55. Eweida AM, Nabawi AS, Abouarab M, Kayed M, Elhammady H, Etaby A, Khalil MR, Shawky MS, Kneser U, Horch RE, Nagy N, Marei MK. Enhancing mandibular bone regeneration and perfusion via axial vascularization of scaffolds. Clin Oral Investig. 2014 Jul;18(6):1671–8. Doi: 10.1007/s00784–013–1143–8. Epub 2013 Nov 19. PMID: 24248640.

Received 06.08.2022
Revised 10.08.2022
Accepted 20.08.2022

INFORMATION ABOUT AUTHORS

Kobets Konstantin Konstantinovich, *Assistant of the department of Oral and Maxillofacial Surgery and Surgical Dentistry of the Medical Institute of Peoples Friendship University of Russia (RUDN University). ORCID: https://orcid.org/0000-0002-8141-0460, SPIN-code: 8706–7429. Tel. +79150999889; e-mail: kobetskonstantin@gmail.com*

Kazaryan Artak Artyomovich, *the 4-th grade student of the Dental Faculty of the Medical Institute of Peoples' Friendship University of Russia. ORCID: https://orcid.org/0000-0003-0669-9353. Tel. +79629392500, e-mail: artak2505@mail.ru*

Bopkhoev Saddam Visingireevich, *Postgraduate student of the department of Oral and Maxillofacial Surgery and Surgical Dentistry of the Medical Institute of the Peoples' Friendship University of Russia (RUDN University). ORCID: https://orcid.org/0000-0003-0431-0033, SPIN-code: 9308–5544. Tel. +79252200108, e-mail: ophoevs@gmail.com*

Cardioplant®

Биоматериалы для управляемой регенерации

Изделия серии bioOST, bioPLATE и FibroMATRIX разработаны инженерами в соответствии с требованиями ведущих отечественных клиницистов. Это материалы для мягкотканой и костной пластики с управляемым поведением и надежным прогнозируемым результатом. Среди нашей линейки Вы сможете найти продукт, необходимый для решения индивидуальной клинической задачи любой сложности.

bioOST

Костные гранулы с коллагеном
XENOGRAFT Collagen
XCol-1-05 | 0.25-1.0 мм | 0.5 см³
XCol-1-1 | 0.25-1.0 мм | 1.0 см³
XCol-1-3 | 0.25-1.0 мм | 3.0 см³
XCol-2-1 | 1.0-2.0 мм | 1.0 см³
XCol-2-3 | 1.0-2.0 мм | 3.0 см³

Костные гранулы без коллагена
XENOGRAFT Mineral
XMn-1-05 | 0.25-1.0 мм | 0.5 см³
XMn-1-1 | 0.25-1.0 мм | 1.0 см³
XMn-1-3 | 0.25-1.0 мм | 3.0 см³
XMn-2-1 | 1.0-2.0 мм | 1.0 см³
XMn-2-3 | 1.0-2.0 мм | 3.0 см³

Кортикальные гранулы
XENOGRAFT Cortical
XCr-1-05 | 0.5-1.0 мм | 0.5 см³
XCr-1-1 | 0.5-1.0 мм | 1.0 см³

Губчатый блок CUBE Collagen
Cb-10 | 20x10x10 мм

Кортикальная пластина
CORTICAL Lamina
Cl-25 | 25x25x1 мм

Кортикальная мембрана
CORTICAL Membrane
CM-20 | 25x20x0.2 мм

bioPLATE

Мембрана bioPLATE Barrier
MB-15 | 15x20 мм
MB-25 | 25x25 мм
MB-30 | 30x40 мм

Мембрана bioPLATE Contur
MBC-15 | 15x20 мм
MBC-25 | 25x25 мм
MBC-30 | 30x40 мм

Коллагеновый 3D-матрикс
FibroMATRIX
FB-15 | 15x20 мм
FB-30 | 30x40 мм
FB-8 | 8 мм

ООО «Кардиоплант»
Пенза, ул. Центральная, 1в, к.2
info@cardioplant.ru
+7 8412 20-58-24
cardioplant.ru